nature COMMUNICATIONS

ARTICLE

Received 26 Apr 2014 | Accepted 4 Feb 2015 | Published 9 Mar 2015

DOI: 10.1038/ncomms7514 OPEN

TLR9 signalling in microglia attenuates seizure-induced aberrant neurogenesis in the adult hippocampus

Taito Matsuda[1], Naoya Murao[1,2], Yuki Katano[1,2], Berry Juliandi[1,3], Jun Kohyama[4], Shizuo Akira[5,6], Taro Kawai[7] & Kinichi Nakashima[1]

Pathological conditions such as epilepsy cause misregulation of adult neural stem/progenitor populations in the adult hippocampus in mice, and the resulting abnormal neurogenesis leads to impairment in learning and memory. However, how animals cope with abnormal neurogenesis remains unknown. Here we show that microglia in the mouse hippocampus attenuate convulsive seizure-mediated aberrant neurogenesis through the activation of Toll-like receptor 9 (TLR9), an innate immune sensor known to recognize microbial DNA and trigger inflammatory responses. We found that microglia sense self-DNA from degenerating neurons following seizure, and secrete tumour necrosis factor-α, resulting in attenuation of aberrant neurogenesis. Furthermore, TLR9 deficiency exacerbated seizure-induced cognitive decline and recurrent seizure severity. Our findings thus suggest the existence of bidirectional communication between the innate immune and nervous systems for the maintenance of adult brain integrity.

[1] Department of Stem Cell Biology and Medicine, Graduate School of Medical Sciences, Kyushu University, 3-1-1 Maidashi, Higashi-ku, Fukuoka 812-8582, Japan. [2] Laboratory of Gene Regulation Research, Graduate School of Biological Sciences, Nara Institute of Science and Technology (NAIST), Nara 630-0192, Japan. [3] Department of Biology, Bogor Agricultural University, Bogor 16144, Indonesia. [4] Department of Physiology, School of Medicine, Keio University, 35 Shinanomachi, Shinjuku-ku, Tokyo 160-8582, Japan. [5] Laboratory of Host Defense, World Premier International Immunology Frontier Research Center, Osaka University, Osaka 565-0871, Japan. [6] Department of Host Defense, Research Institute for Microbial Diseases, Osaka University, Osaka 565-0871, Japan. [7] Laboratory of Molecular Immunobiology, Graduate School of Biological Sciences, NAIST, Nara 630-0192, Japan. Correspondence and requests for materials should be addressed to K.N. (email: kin1@scb.med.kyushu-u.ac.jp).

Adult neural stem/progenitor cells (aNS/PCs) in the subgranular zone (SGZ) of the adult hippocampal dentate gyrus (DG) proliferate and give rise to new neurons continuously throughout life to maintain proper brain functions[1]. Although this homoeostatic neurogenesis is strictly controlled under normal physiological conditions, misregulation of aNS/PCs leads to aberrant neurogenesis and impairment of hippocampal-dependent learning and memory under pathological conditions such as stress, depression, ischaemia and epilepsy[2]. The aNS/PC niche, a microenvironment comprising various components including blood vessels, neurons, astrocytes and microglia, is known to contribute to different aspects of neurogenesis under both normal and pathological conditions[2–7]. However, how it responds to pathological conditions to rectify any aberrant behaviour of aNS/PCs is yet to be elucidated.

Microglia, the major immune cell type in the brain, remove dying cells and cellular debris without inducing inflammation under physiological conditions[8]. In response to pathological insults such as infection or brain injury, activated microglia accumulate in the injured site and secrete pro- and/or anti-inflammatory cytokines[9,10]. In addition to these functions, increasing evidence suggests that microglia play important roles in aNS/PC regulation under physiological conditions[11–13].

Toll-like receptors (TLRs) are innate immune receptors that recognize pathogen- or damage-associated molecular patterns (P/DAMPs)[14–16], and provide an important machinery by which microglia can sense both pathogen- and host-derived ligands and consequently secrete pro- and/or anti-inflammatory cytokines. While TLR2 and TLR4 have been implicated in adult hippocampal neurogenesis under physiological conditions[17], it is completely unknown whether the nucleic acid-sensing TLR7 and TLR9 can also regulate neurogenesis. To elucidate the functions of these TLRs is important, particularly in pathological conditions, because nucleic acids released from endogenous damaged cells could activate them, resulting in the misregulation of aNS/PC behaviour.

We report here that the loss of TLR9 but not TLR7 reduced seizure-mediated sustained microglial activation and tumour necrosis factor-alpha (TNF-α) production in the hippocampus. Pharmacological inhibition of microglial activation or TNF-α production in wild-type (WT) mice exacerbated aberrant neurogenesis to a similar extent to that observed in TLR9 knockout (KO) mice after seizure. Furthermore, conditioned medium (CM) from hyperactivated hippocampal neurons upregulated *Tnf-α* expression in primary cultures of WT but not TLR9 KO microglia, and this effect was completely abolished when the CM was pretreated with DNase. These results indicate that microglia are activated through TLR9 signalling triggered by self-DNA derived from seizure-induced degenerating neurons in the hippocampus, leading to a sustained expression of TNF-α which attenuates the induced aberrant neurogenesis.

Results

TLR9 deficiency aggravates aberrant neurogenesis. We found that Iba1-positive microglia were in close proximity to about 80% of aNS/PCs (positive both for green fluorescent protein (GFP) expressed under the promoter of the NS/PC marker gene *Sox2* and for the aNS/PC marker glial fibrillary acidic protein (GFAP)) in the SGZ of the hippocampus under both physiological and pathological conditions (Supplementary Fig. 1a–c), implying that niche-resident microglia activated in response to pathological insults also affect the behaviour of aNS/PCs by producing pro- and/or anti-inflammatory cytokines.

As a first step towards understanding the roles of TLR7 and TLR9, we confirmed their expression in microglia and found that they are much more highly expressed in these cells than in other neural cell types including NSCs (Supplementary Fig. 1d). To investigate the role of TLR7 and TLR9 in adult hippocampal neurogenesis, we injected bromodeoxyuridine (BrdU) once a day for 7 days into physiologically normal 8-week-old WT, TLR7-KO and TLR9-KO mice to label proliferating aNS/PCs in the DG and killed the mice 1 day after the final injection. We observed no significant difference among these mice (Fig. 1a–c), since TLR signalling is activated by P/DAMPs only under pathological conditions[15,16]. Although we have previously reported that convulsive seizure induces aberrant neurogenesis in the adult DG[18], how animals respond to this pathological condition remains unknown. We thus sought to examine the effects of TLR7 and TLR9 deficiency on the response to convulsive seizure induction. To induce the seizure, we administered kainic acid (KA), a potent glutamate analogue that triggers neuronal

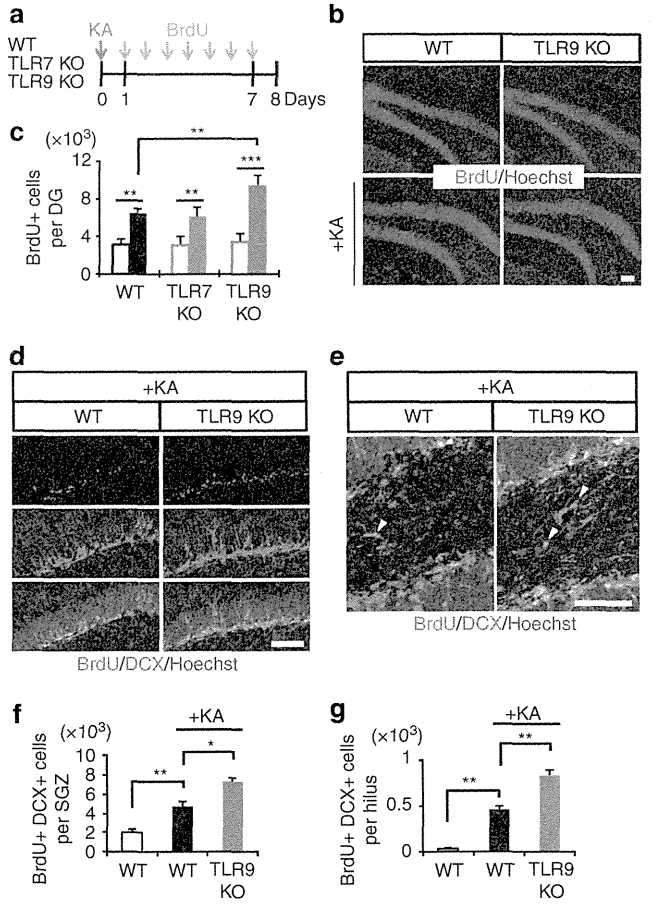

Figure 1 | TLR9 deficiency aggravates seizure-induced aberrant neurogenesis. (**a**) Experimental timeline for assessing aNS/PC proliferation in WT, TLR7-KO and TLR9-KO mice. (**b**) Representative images of the DG and stained with BrdU (red) and Hoechst (blue) showed that KA-induced proliferation of aNS/PCs in TLR9-KO mice was more extensive than in WT mice. Scale bar, 50 μm. (**c**) Quantification of total number of BrdU-positive (BrdU+) cells in the DG with (filled bars) or without (open bars) KA treatment. After seizure, the number of BrdU+ cells was higher in TLR9-KO mice than in WT mice ($n=5$ animals). (**d**,**e**) Representative images of BrdU (red) and DCX (green) double-labelled (BrdU+DCX+) newly generated neurons in the SGZ (**d**) and the hilus (**e**) ($n=5$ animals). Scale bars, 50 μm. White arrowheads indicate new neurons located ectopically in the hilus. (**f**,**g**) Quantification of the number of BrdU+DCX+ cells in **c** (SGZ, **f**) and **e** (hilus, **g**; $n=5$ animals). $^{*}P<0.05$, $^{**}P<0.01$ and $^{***}P<0.001$ by analysis of variance with Tukey *post-hoc* tests.

hyperactivation, intraperitoneally to WT, TLR7-KO and TLR9-KO mice. KA-induced acute convulsive seizure is known to trigger aberrant augmentation of neurogenesis in the DG and the migration of newborn neurons to ectopic locations such as the hilus, resulting in the impairment of hippocampus-dependent memory[3,18,19]. Consistent with previous reports, we observed a significant increase in the number of BrdU-positive cells within the SGZ in all KA-treated mice (Fig. 1a–c). Interestingly, while the number of BrdU-positive cells within the SGZ at 1 week after KA administration did not differ between WT and TLR7-KO mice, the number was higher in TLR9-KO mice (Fig. 1a–c). In addition, an increased number of BrdU-retaining and doublecortin (DCX, an immature neuron marker)-expressing newly generated and immature neurons was observed in the DG, including both the SGZ and the hilus, of TLR9-KO mice (Fig. 1d–g), suggesting that the loss of TLR9 stimulates KA-induced aberrant neurogenesis. We decided to focus on TLR9-KO mice in the following experiments because neurogenesis in TLR7-KO mice was indistinguishable from that in WT mice even in the pathological condition.

We further traced the differentiation and survival of newly generated cells in the DG at 3 weeks after the last BrdU injection (Fig. 2a). The TLR9-KO mice showed a higher number of BrdU-retaining cells in the DG than that in WT mice (Fig. 2b,d), and the majority of BrdU-retaining cells had become positive for the mature neuronal marker NeuN (Fig. 2b–e). However, the loss of TLR9 had no effect on the proportion of NeuN-positive neurons among BrdU-positive cells. Concordant with the increase in BrdU-positive cells, the number of newly generated S100β- or GFAP-positive astrocytes also increased in the DG of TLR9-KO compared with WT mice (Fig. 2b–e), suggesting that aNS/PC differentiation *per se* was not affected by the loss of TLR9 as shown in Fig. 2f for neuronal differentiation as an example. Furthermore, we measured the proportion of surviving total BrdU-positive cells in WT and TLR9-KO mice. To calculate the ratio of surviving cells after seizure, we divided the total number of BrdU-positive cells at 3 weeks after the last BrdU injection by that at 1 day after the last BrdU injection. We found no difference in the survival ratio (Fig. 2g), indicating that TLR9 signalling does not contribute to the survival of newborn cells in the DG. Taken together, these results suggest that TLR9 deficiency aggravates seizure-induced aberrant neurogenesis in the hippocampus by promoting aNS/PC proliferation. In other words, these data indicate that TLR9 signalling attenuates seizure-induced abnormal proliferation of aNS/PCs to maintain homoeostatic neurogenesis in the DG.

Activated microglia attenuates aberrant neurogenesis. Before further analyzing TLR9 function, we determined whether TLR9 is indeed expressed in microglia in the DG *in vivo*. As shown in Supplementary Fig. 1e, Iba1-positive microglia clearly expressed TLR9. We also examined whether i.p. KA injection compromises the integrity of the blood–brain barrier (BBB) by using Evans blue dye, because macrophages infiltrate the damaged brain in conditions such as ischaemia through a disrupted BBB. However, Evans blue dye leakage was not found in the brain, while the dye was detected in other organs in both WT and TLR9-KO mice, indicating that the BBB remains intact after KA injection in these mice (Supplementary Fig. 1f). Although we cannot completely exclude the possibility that macrophages infiltrate the brain after seizure through the intact BBB, any such macrophage population would be exceedingly small compared with the brain-resident microglia. We therefore focused mainly on microglia as TLR9-expressing cells in this study.

Since it has been shown that epileptic seizure induces microglial activation in the hippocampus[20], we evaluated the microglial activation status in WT and TLR9-KO DG after seizure by immunohistochemistry with an antibody against CD68, which is upregulated in activated microglia (Supplementary Fig. 2a,b). Many CD68-positive activated microglia were detected in WT mice 7 days after seizure, whereas the activation was much lower

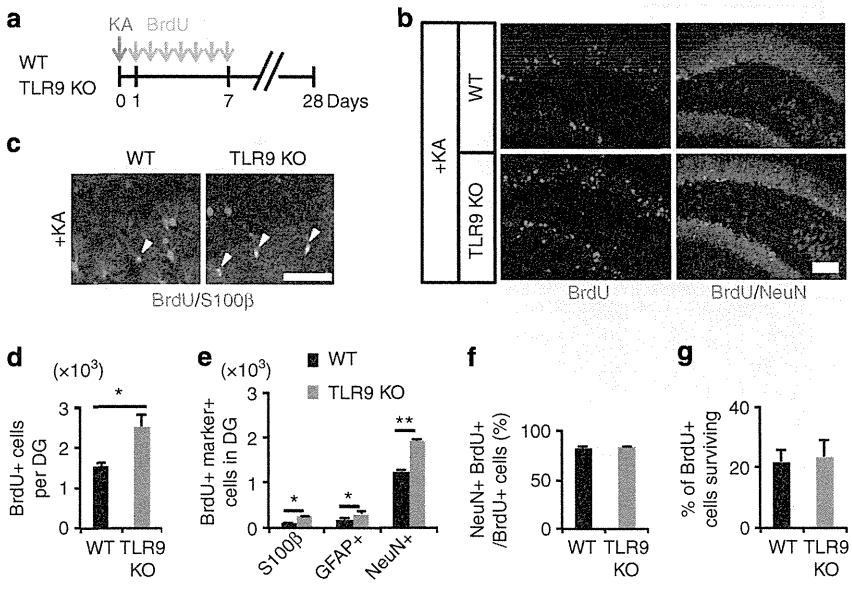

Figure 2 | Loss of TLR9 increases newly generated mature neurons after seizure. (**a**) Experimental scheme for examining the number of newly generated mature neurons. (**b**) Representative images of staining for NeuN (green) and BrdU (red) in the DG ($n=5$ animals). Scale bar, 50 μm. (**c**) Representative images of BrdU (red) and S100β (green) staining in the DG of KA-administered WT and TLR9-KO mice. White arrowheads indicate BrdU and S100β double-labelled newborn astrocytes. Scale bar, 50 μm. (**d**,**e**) The DG of TLR9 KO mice exhibited increased numbers of BrdU+ cells (**d**) and newly generated BrdU+NeuN+ mature neurons (**e**) ($n=5$ animals). (**f**,**g**) Quantification of BrdU+ cells for assessing differentiation (**f**) and survival (**g**) of newly generated cells in the DG ($n=5$ animals). (**d**) $^{*}P<0.05$ by Student's *t*-test. (**e**) $^{*}P<0.05$ and $^{**}P<0.01$ by analysis of variance with Tukey *post-hoc* tests.

in TLR9-KO mice, indicating that sustained microglial activation in the DG requires functional TLR9 (Fig. 3a). This result prompted us to ask whether TLR9-mediated microglial activation inhibits aNS/PC proliferation. To induce microglial activation, we prepared primary cultured microglia (Supplementary Fig. 3a) and stimulated them *in vitro* with the TLR9 ligand ODN1585. Incubation of microglia with ODN1585 upregulated the expression of two well-known targets of TLR signalling, *Tnf-α* and *Interferon* (*Ifn*) β, in a dose-dependent manner (Supplementary Fig. 3b). We then tested whether the CM of microglia activated with ODN1585 affects aNS/PC proliferation, and found that it decreased aNS/PC proliferation compared with control CM without affecting cell survival (Fig. 3b–d). We also performed experiments using different ligands (ODN2395 and ODN1826) for TLR9, and found that CM from microglia activated with these two ligands likewise inhibited aNS/PC proliferation (Supplementary Fig. 4). These data indicate that microglia activated through TLR9 inhibit aNS/PC proliferation *in vitro*.

Minocycline, a semisynthetic tetracycline derivative, is known to inhibit microglial activation *in vivo*[21]. To inhibit sustained microglial activation after seizure, we injected minocycline intraperitoneally into WT and TLR9-KO mice once daily for 8 consecutive days. We confirmed that seizure-induced microglial activation was inhibited by minocycline treatment (Supplementary Fig. 2b). When we inhibited microglial activation with minocycline in KA-administered WT mice, seizure-induced aberrant neurogenesis was exacerbated, reaching a level similar to

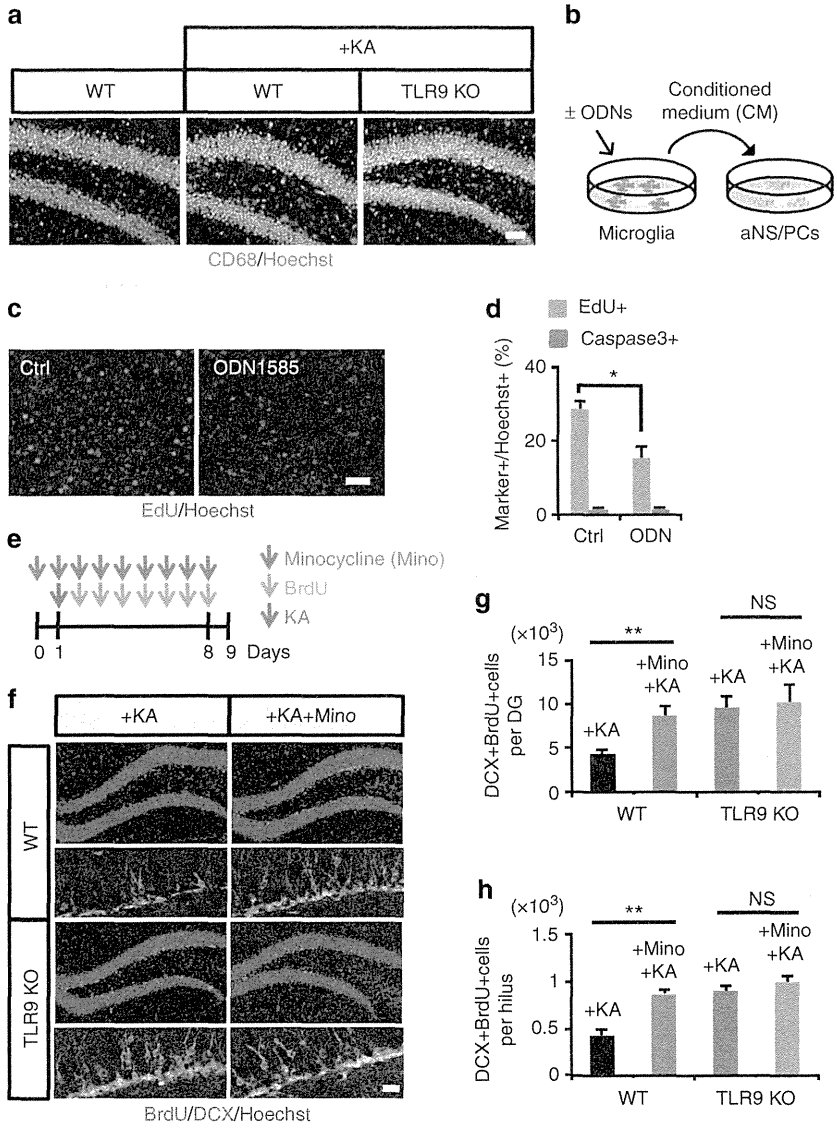

Figure 3 | Activated microglia attenuates aberrant neurogenesis. (**a**) Representative images of CD68+ (magenta) activated microglia in the DG of TLR9 KO and WT mice with or without KA treatment ($n=4$ animals). Scale bar, 50 μm. (**b**) Experimental scheme for assessing aNS/PC proliferation in the presence or absence of CM derived from ODN1585-stimulated microglia. (**c**) Representative images of EdU (red) and Hoechst (blue) staining of aNS/PCs cultured with CM of ODN1585-treated (right) and untreated (left) microglia as a control (Ctrl) ($n=5$ experiments). Scale bar, 50 μm. (**d**) Quantification of EdU+ Hoechst+ cells or an apoptotic cell marker active caspase3+ Hoechst+ cells. ODN1585-dependent microglial activation inhibits aNS/PCs without affecting cell survival ($n=5$ experiments). (**e**) Experimental scheme for assessing aNS/PC proliferation in minocycline-treated mice. (**f**) Representative images of BrdU+ (red) DCX+ (green) newly generated neurons in the DG. Scale bar, 50 μm. (**g**,**h**) Quantification of the number of BrdU+ DCX+ cells in the DG (**g**) and hilus (**h**) ($n=5$ animals). Ectopic neurogenesis increased in minocycline-treated mice to a similar extent to that observed in TLR9 KO mice ($n=5$ animals). (**d**) $^{*}P<0.01$ by Student's *t*-test. (**g**,**h**) NS means not significant ($P>0.05$). $^{*}P<0.05$, $^{**}P<0.01$ by analysis of variance with Tukey *post-hoc* tests.

that observed in TLR9-KO mice treated with KA alone (Fig. 3e–h). Furthermore, there were no differences in the number of BrdU- and DCX-positive cells (newly generated neurons) between minocycline-treated or -untreated TLR9-KO mice after seizure (Fig. 3f–h). Taken together, these results suggest that activated microglia attenuate seizure-induced neurogenesis through TLR9 signalling. Minocycline itself did not affect neurogenesis under normal physiological conditions (Supplementary Fig. 2c–e).

Microglia-derived TNF-α alleviates aberrant neurogenesis. Recent studies have shown that various inflammation-related molecules regulate adult neurogenesis in the DG[22–24], leading us to hypothesize that such molecules released from activated microglia might attenuate aberrant neurogenesis induced by seizure. To test this, we performed quantitative real-time PCR (qRT–PCR) analysis. At one day after seizure induction, expression of inflammatory cytokines, such as *Il-1β*, *Il-6* and *Tnf-α*, in both WT and TLR9-KO DG was upregulated compared to KA-untreated controls (Fig. 4a and Supplementary Fig. 5). Intriguingly, the higher expression level of *Tnf-α* and not other mRNAs was sustained in KA-treated WT mice at 4 or 7 days after seizure, yet the *Tnf-α* expression level in TLR9-KO mice reverted to the control level by 4 days after seizure induction (Fig. 4a). Given that TNF-α has previously been shown to suppress neurogenesis in the DG[23], we tested whether TNF-α inhibits aNS/PC proliferation *in vitro*, and found that it did so in a dose-dependent manner (Supplementary Fig. 6a,b). We also examined whether IL-12 and IFN-γ inhibit aNS/PC proliferation, because their expression differed between WT and TLR9-KO mice at day 1 after seizure (Supplementary Fig. 5). However, we found no difference in the number of EdU (a thymidine analogue)-positive cells irrespective of IL-12 and IFN-γ treatment, suggesting that aNS/PC proliferation is unaffected by these cytokines (Supplementary Fig. 6c–f). Therefore, we decided to focus on TNF-α in subsequent experiments. To examine whether TLR9 signalling-mediated TNF-α production by microglia inhibits aNS/PC proliferation, we pretreated CM samples from microglia with a TNF-α-neutralizing antibody or immunoglobulin-G (IgG) control, and added them to aNS/PC cultures (Fig. 4b). ODN1585-untreated microglial CM pretreated with the TNF-α antibody did not affect aNS/PC proliferation. In marked contrast, the anti-proliferative effect of the CM from ODN1585-treated microglia was abolished with the TNF-α antibody, indicating that TLR9 stimulation-induced TNF-α is the factor responsible for the inhibition of aNS/PC proliferation (Fig. 4c,d).

Thalidomide is known as a BBB-permeable inhibitor of TNF-α production[25]. To allow administered thalidomide enough time to be fully effective in inhibiting *Tnf-α* expression by the time of KA injection, we started the injection of thalidomide into WT mice 1 day before the KA injection, and continued once daily until 3 days after seizure; the mice were then killed 4 days after seizure. As shown in Supplementary Fig. 6g,h, we found that thalidomide treatment suppressed *Tnf-α* expression in the DG of WT mice 4 days after seizure. When we injected thalidomide into WT mice once daily for 8 consecutive days, in accordance with our *in vitro* experiments, suppression of TNF-α production aggravated aberrant neurogenesis *in vivo* as observed in thalidomide-untreated TLR9-KO mice after seizure (Fig. 4e–h).

Next, to understand more precisely the behaviour of aNS/PCs in response to seizure, we examined aNS/PC proliferation at earlier time points after KA administration in both WT and TLR9-KO mice. After 1, 2, 3 and 4 days of KA administration, we injected BrdU into these mice every 4 h (four times) and killed them 12 h after the last BrdU injection (Supplementary Fig. 7a). We found that the number of BrdU-positive cells which were proliferating at day 4 after seizure induction in WT mice was significantly higher than in untreated WT mice (Supplementary Fig. 7b,d). In contrast, statistically different BrdU-positive cell numbers between untreated and KA-treated mice were already observed at day 2 in TLR9-KO mice (Supplementary Fig. 7b,d). Moreover, these trends of increased BrdU-positive cell numbers in WT and TLR9-KO mice were inversely correlated with the degree of microglial activation and *Tnf-α* expression in these mice (Supplementary Fig. 7c,e). As shown in Supplementary Fig. 7e, a dramatic upregulation of *Tnf-α* expression in both WT and KO mice was observed at day 1 after KA injection, probably attributable to a direct effect of KA. By 2 days, *Tnf-α* expression in KA-injected TLR9-KO mice had already reverted to a level similar to that in the control, but was still high in KA-injected WT mice, suggesting that the difference was attributable to TLR9 deficiency. To confirm the effectiveness of thalidomide on the inhibition of *Tnf-α* expression, we then injected thalidomide into WT mice 1 day before the difference in *Tnf-α* expression between WT and TLR9 KO mice became apparent (day 2) (Supplementary Fig. 8a). As shown in Supplementary Figs 7d and 8c, BrdU-positive cells had not yet increased in response to KA treatment at day 3 in WT mice, but we did observe an increase of BrdU-positive cells in response to thalidomide treatment (Supplementary Fig. 8b,c). We then examined whether TNF-α reduces exacerbated neurogenesis in TLR9-KO mice after seizure. We infused recombinant TNF-α protein into the DG of TLR9-KO mice after seizure (Supplementary Fig. 9a) and found that TNF-α indeed reduced the seizure-induced aberrant neurogenesis in these mice (Supplementary Fig. 9b,c). Taken together, these results indicate that TLR9 signal-regulated TNF-α production by microglia is a critical process to withstand the aberrant neurogenesis following seizure.

TLR9 signalling does not affect localization of new neurons. Having shown that TLR9-dependent TNF-α production in microglia attenuates seizure-induced aNS/PC proliferation and ectopic generation of new neurons, we next asked whether TLR9 signalling affects the location of DCX-positive newly generated neurons in the DG at 8 days after seizure. The loss of TLR9 had no effect on the distribution of DCX-positive neurons, whereas the number of DCX-positive neurons in each area examined was increased in TLR9-KO mice after seizure compared with WT mice (Supplementary Fig. 10a–c). Since microglia activation and TNF-α production are important processes downstream of TLR9 signalling, minocycline and thalidomide treatment did not affect the distribution but did increase the number of DCX-positive cells, similar to TLR9 loss (Supplementary Fig. 10b). We also examined the morphology of DCX-positive cells after seizure by Sholl analysis and measurement of dendrite length. TLR9-KO mice showed no significant differences in these analyses, although KA itself affected the morphology of DCX-positive neurons (Supplementary Fig. 11a–c). Thus, these data indicate that TLR9 deficiency aggravates seizure-induced aberrant neurogenesis in the hippocampus by promoting aNS/PC proliferation.

Loss of TLR9 worsens seizure-induced behavioural impairments. We have previously shown that seizure-induced aberrant neurogenesis impairs a hippocampal-dependent cognitive function[18]. Since seizure-induced aberrant neurogenesis is exacerbated in TLR9-KO mice, we examined whether KA-treated TLR9-KO mice show further cognitive decline by subjecting KA-treated or -untreated WT and TLR9-KO mice to a hippocampus-dependent place recognition task (Fig. 5a). Administration of KA to WT mice induced cognitive decline in agreement with our previous

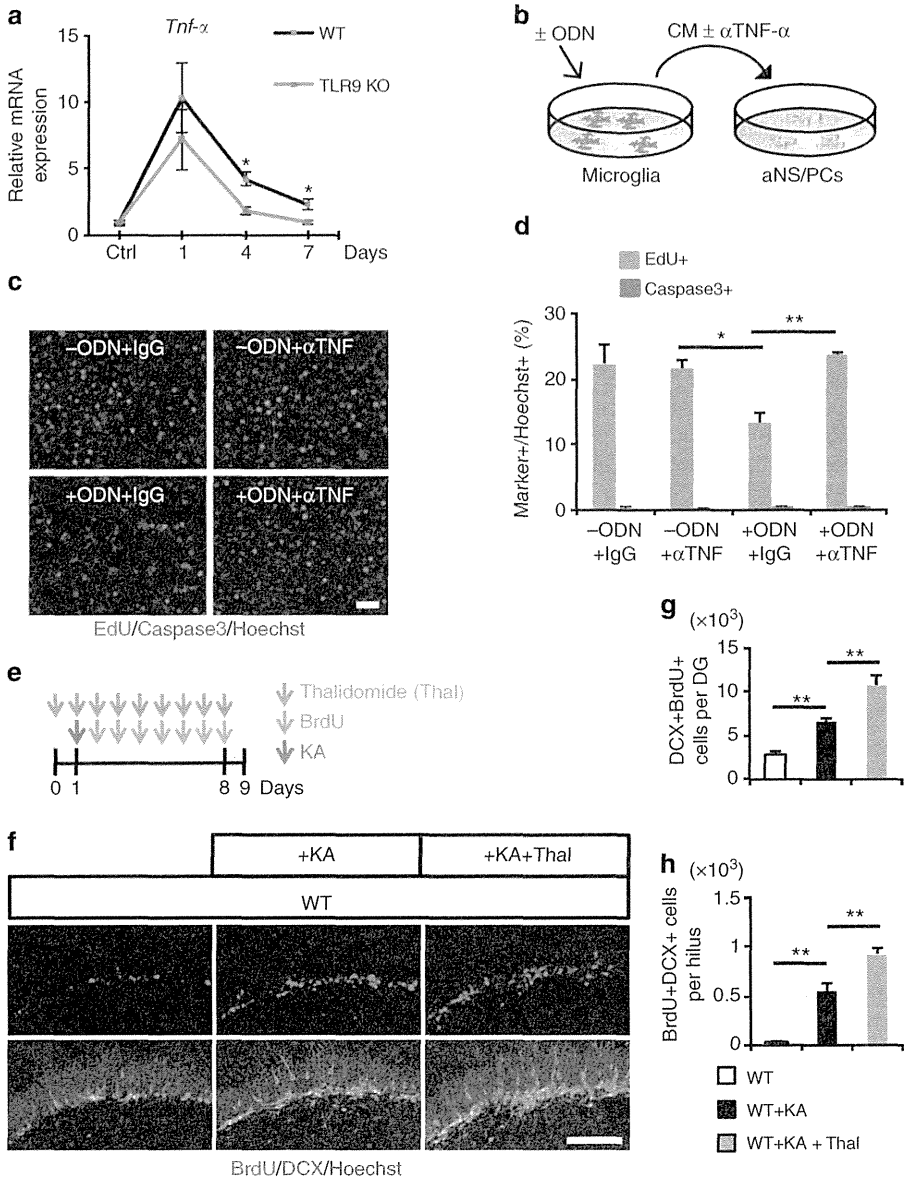

Figure 4 | Microglia-derived TNF-α alleviates aberrant neurogenesis. (**a**) qRT-PCR analyses of *Tnf-α* levels in the DG of WT and TLR9 KO mice at the indicated time points after seizure. Experimental controls were KA-untreated WT and TLR9 KO mice, respectively ($n=3$ animals). $^{*}P<0.05$ by analysis of variance (ANOVA) with Tukey *post-hoc* tests. (**b**) Experimental scheme for assessing aNS/PC proliferation in microglia culture-derived CM pretreated with TNF-α-neutralizing antibody or IgG control. (**c**) Representative images of EdU (red), active caspase3 (green) and Hoechst (blue) staining in aNS/PCs cultured with the indicated CM from microglia ($n=4$ experiments). Scale bar, 50 μm. (**d**) Quantification of EdU+ or active caspase3+ cells in **c** ($n=4$ experiments). (**e**) Experimental timeline for assessing aNS/PC proliferation in thalidomide (Thal)-treated mice. (**f**) Representative images of BrdU+DCX+ newly generated immature neurons in the DG ($n=4$ animals). Scale bar, 50 μm. (**g**,**h**) Quantification of the number of BrdU+DCX+ cells in **f**, in the DG (**g**) and in the hilus (**h**) ($n=4$ animals). $^{*}P<0.05$ and $^{**}P<0.01$ by ANOVA with Tukey *post-hoc* tests.

report[18] (Fig. 5b). Moreover, the loss of TLR9 aggravated this seizure-induced cognitive decline, although without KA treatment WT and TLR9-KO mice showed no significant difference in the test (Fig. 5b). When we inhibited microglial activation in WT mice treated with KA using minocycline, the level of impairment in these mice decreased to an extent similar to that observed in TLR9-KO mice without treatment (Fig. 5b). These data suggest that TLR9-mediated microglial activation attenuates seizure-induced cognitive decline in WT mice.

A recent study has indicated that ectopically located new neurons contribute to epileptogenesis[26]. This observation prompted us to examine whether either TLR9 deficiency or inhibition of microglia activation by minocycline affect the severity of seizure induced by KA re-injection at 48 days after the first KA injection (Fig. 5c). All mice showed no difference in scores of seizure following the first KA injection (Fig. 5d,e). Furthermore, the first administration of KA at low concentration did not affect the scores in WT or TLR9-KO mice (Supplementary Fig. 12a,b). However, when we re-injected KA at low concentration to TLR9-KO mice 48 days after the first KA injection, they developed more severe seizures compared with WT mice (Fig. 5f,g). Minocycline treatment indeed aggravated the symptoms in WT mice, *albeit* to a lesser extent than that observed in TLR9 KO mice without minocycline, probably because we ceased minocycline treatment at 7 days after the first KA injection. During the 7 days after the first KA administration, microglial activation was inhibited by minocycline, but resumed after the cessation of this treatment. We therefore inferred that

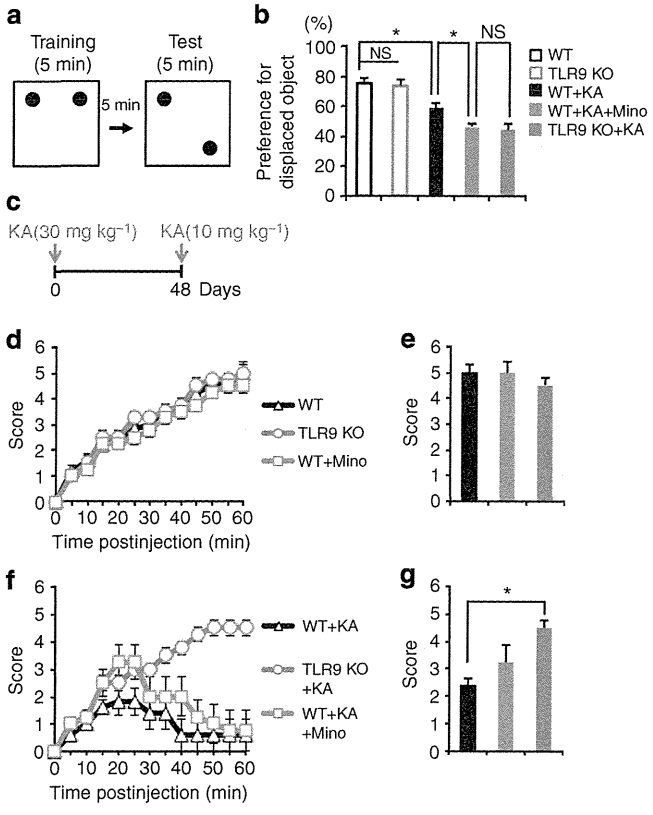

Figure 5 | TLR9 deficiency worsens seizure-induced behavioural impairments. (**a**) Schematic paradigm of place recognition test. Five minutes after training phase, mice were allowed to explore two objects one of which was displaced to different location from the original location. (**b**) KA-treated WT mice did not show much preference for the displaced object compared with untreated WT mice. This cognitive decline was exacerbated in TLR9 KO mice. KA-treated WT mice that received minocycline treatment showed the similar level of preference for the displaced object as KA-treated TLR9-KO mice did. Each group has eight mice. NS means not significant ($P>0.05$). *$P<0.05$ by analysis of variance (ANOVA) with Tukey *post-hoc* tests. (**c**) Experimental scheme for examining recurrent seizure severity. All mice were administrated with KA (10 mg kg^{-1}) 48 days after first KA injection (30 mg kg^{-1}). (**d**) Seizure response over time in WT, TLR9 KO and minocycline-treated WT mice following the first KA injection (30 mg kg^{-1}) ($n=8$ animals). For each 5-min interval, the highest level of seizure activity was scored using previously described scale (see Methods). (**e**) The maximum score of each mouse group during the 60-min trial in **d**. (**f**) Seizure response over time in WT mice, TLR9 KO mice and minocycline-treated WT mice following KA injection (10 mg kg^{-1}) 48 days after first KA injection ($n=8$ animals). (**g**) The maximum score of each mouse group during the 60-min trial in **f**. *$P<0.01$ by ANOVA with Tukey *post-hoc* tests.

the inhibition of aberrant neurogenesis was less effective in minocycline-treated WT mice than in untreated WT mice. Taken together, these results suggest that TLR9 signalling attenuates seizure-induced cognitive decline and recurrent seizure severity.

Degenerating neuron-derived DNA activates TLR9 signalling. Finally, we addressed the possibility that an endogenous cell-derived ligand activates TLR9 signalling in microglia after seizure. Increasing evidence indicates that, in addition to detection of PAMPs, TLRs contribute to the detection of damage to the CNS by recognizing endogenous DAMPs released from dying or degenerating cells[15,16,27]. As we have shown previously[18], seizure causes neuronal degeneration in the DG. We collected CM from

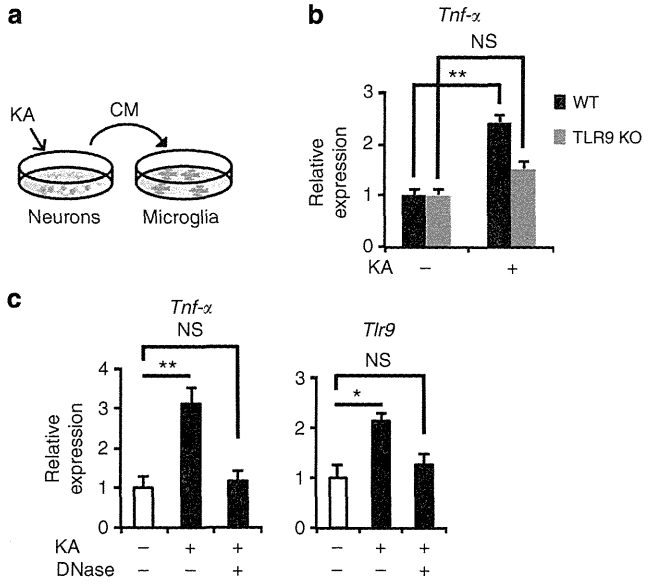

Figure 6 | Degenerating neuron-derived DNA activates TLR9 signalling. (**a**) Experimental scheme for the identification of an endogenous ligand for TLR9 expressed in microglia. (**b**) qRT-PCR analyses of *Tnf-α* levels in microglia from WT and TLR9 KO mice 12 h after incubation with CM from KA-treated or -untreated neurons. TLR9 KO microglia failed to induce *Tnf-α* expression in response to CM from KA-treated neurons ($n=4$ experiments). (**c**) qRT-PCR analyses of *Tnf-α* expression levels in microglia from WT mice 12 h after incubation with DNase-pretreated CM from KA-treated neurons ($n=5$ experiments). NS means not significant ($P>0.05$). *$P<0.05$ and **$P<0.01$ by ANOVA with Tukey *post-hoc* tests.

hippocampal neurons stimulated with KA, and cultured primary microglia in its presence for 12 h (Fig. 6a). We found that the *Tnf-α* expression level in primary WT microglia was increased by the CM of KA-treated neurons. In contrast, the CM failed to induce *Tnf-α* expression in TLR9-KO microglia (Fig. 6b). When we pretreated the CM from KA-treated neurons with DNase, the CM-induced elevation of *Tnf-α* expression in primary microglia was abolished (Fig. 6c). These data suggest that DNA derived from degenerating neurons activates TLR9 signalling in microglia as an endogenous ligand. Moreover, we observed that the CM of KA-treated neurons upregulated the expression of *Tlr9* in primary microglia, indicating the existence of a positive feedback loop to enhance TLR9 signalling in microglia (Fig. 6c). CM-induced *Tlr9* expression was also severely compromised by pretreatment with DNase.

The TLR9 signalling pathway is known to activate NF-κB, which controls the expression of inflammatory cytokine genes[28]. We examined whether CM from degenerating neurons induces NF-κB activation in microglia via TLR9. When we cultured microglia with CM derived from KA-stimulated hippocampal neurons, p65 protein, a subunit of the NF-κB complex, translocated into the nucleus, indicating that the CM can indeed activate NF-κB in microglia (Supplementary Fig. 13a,b). This activation was abolished by DNase or TLR9 inhibitor (ODN2088) treatment (Supplementary Fig. 13a,b). These data suggest that DNA derived from degenerating neurons evokes NF-κB activation in microglia via TLR9.

Discussion

TLR9 was initially identified as a receptor that recognizes microbial DNA[29], but current research has shown that TLR9 can sense self-DNA as a DAMP[30], and it appears to be involved in numerous immune processes and autoimmune diseases[14].

However, it is unknown whether TLR9 senses self-DNA to modulate CNS function in the absence of pathogen-derived DNA. In the present study, we have suggested that TLR9 senses self-DNA from degenerating hippocampal neurons to attenuate seizure-induced aberrant neurogenesis, revealing a role for TLR9 in maintaining brain integrity. TLR7-KO mice, in contrast, displayed no impaired phenotype, at least in neurogenesis. Moreover, when we pretreated CM from KA-treated neurons with RNase to deplete TLR7 ligand (RNA), the CM-induced elevation of *Tnf-α* expression in primary microglia was not abolished (Supplementary Fig. 14). These data suggest that self-RNA from degenerating neurons does not function as a TLR7 ligand for the regulation of neurogenesis following seizure, although TLR7 is known to recognize self-RNA and microRNA[31,32]. The microRNA let-7, a highly abundant regulator of gene expression in the CNS, activates TLR7 in neurons and induces neurodegeneration[31]. Neuronal TLR7 is also reported to sense self-RNA derived from neighbouring cells and thus to impair axonal outgrowth of cortical neurons[32]. These observations warrant further experimentation using TLR7-KO and/or a double-KO with TLR9 to gain a better understanding of how immune receptors recognize endogenous ligands from neighbouring CNS cells and modulate brain functions.

We have shown that the activation of TLR9 signalling in microglia induces TNF-α expression, resulting in the attenuation of aberrant neurogenesis in the hippocampus. Consistent with our findings, it has been reported that TNF receptor 1 (TNFR1) expressed in aNS/PCs is a negative regulator for adult hippocampal neurogenesis[23]. The loss of TNFR1 enhances seizure-mediated aNS/PC proliferation and increases neurogenesis in the hippocampus. TNF-α is a key factor in the immune response[33], but it is unclear whether TNF-α has any positive effects in the CNS since many studies have focused on its roles as a negative effector in neurodegenerative disorders such as Alzheimer's disease[34]. Thus, our results unveil a positive aspect of TNF-α function in the CNS for the maintenance of homoeostatic neurogenesis.

The findings that microglia are in close proximity to aNS/PCs (Supplementary Fig. 1a–c) and that inhibition of microglial activation after seizure exacerbates aberrant neurogenesis (Fig. 3e–h and Supplementary Fig. 2) highlight the importance of microglia for the regulation of adult neurogenesis in the aNS/PC niche. Consistent with these observations, several previous studies have suggested that microglia inhibit adult hippocampal neurogenesis[12,13]. However, it has also been suggested that activated microglia promote neurogenesis by secreting trypsinogen[35]. These contradictory assertions are probably due to the contribution of different subtypes of activated microglia to the regulation of neurogenesis. Microglia can undergo different modes of polarized activation, which give rise to potentially neurotoxic classic-M1 (characterized by the release of pro-inflammatory factors) or potentially neuroprotective alternative-M2 (characterized by the expression of anti-inflammatory cytokines) subtypes[10,36,37]. In the CNS, increasing evidence indicates that M1 microglia exacerbate neurodegenerative disease through the production of pro-inflammatory cytokines[10]. Minocycline is known as an inhibitor of M1 microglial activation since it selectively inhibits M1 microglia-related gene expression[21]. Therefore, it is plausible that M1 microglia release TNF-α and consequently attenuate seizure-induced aberrant neurogenesis.

In this study, we have identified a novel, intrinsic mechanism to attenuate aberrant neurogenesis that involves interactions between TLR9-expressing immune cells and neural cells. We show that TLR9 signalling activated by DNA from degenerating neurons induces TNF-α production in microglia, resulting in the inhibition of seizure-induced aberrant neurogenesis (Supplementary Fig. 15). Thus, microglia in the aNS/PC niche respond via TLR9 to the insult induced by seizure and ensure homoeostatic neurogenesis. However, we suspect that our proposed mechanism is one among many that contribute to homoeostatic neurogenesis, because the aNS/PC niche is composed of many types of cells and is vulnerable to a variety of pathological stimuli. Future studies will reveal as-yet-unknown mechanisms by which the niche reacts to these stimuli to ensure the maintenance of brain homoeostasis. Boosting the functions of these intrinsic mechanisms should offer therapeutic strategies for diseases associated with abnormal neurogenesis, such as major depression, ischaemia, Alzheimer's disease and epilepsy.

Methods

Animals. All efforts were made to minimize animal suffering and to reduce the number of animals used. Animals were housed on a 12/12-h light/dark cycle and fed *ad libitum*. TLR7-KO and TLR9-KO mice were on a C57BL/6 background. Sox2–GFP mice[38] were a gift from F.H. Gage (Salk Institute, USA). Male 8-week-old mice were used for this study. To induce seizure, the mice received i.p. injections of KA (30 mg kg^{-1}; Enzo Life Sciences) dissolved in saline. Behaviour of KA-treated mice was observed for 1 h after the injection and the seizure score was recorded, according to previously described criteria[39,40]. Briefly, we used the following seizure scale: no response (0), staring and reduced locomotion (1), activation of extensors and rigidity (2), repetitive head and limb movements (3), sustained rearing with clonus (4), loss of posture (5), and status epilepticus and death (6). The scores did not differ between WT and TLR9 KO mice following KA injection. To assess recurrent seizure severity, all mice were re-injected with KA (10 mg kg^{-1}) at 48 days after the first KA injection (30 mg kg^{-1}).

The day after KA injection, BrdU (50 mg kg^{-1}; Sigma) dissolved in saline was injected intraperitoneally into TLR7-KO, TLR9-KO and WT mice daily for 1 week to monitor cell proliferation, differentiation and survival. These mice were killed 1 day or 21 days after the last injection of BrdU. The day before seizure induction, minocycline (20 mg kg^{-1}; Sigma) dissolved in saline was injected intraperitoneally into TLR9-KO and WT mice once daily for 8 consecutive days to inhibit microglial activation. To inhibit seizure-induced TNF-α production, thalidomide (250 mg kg^{-1}; Sigma) dissolved in 0.5% carboxymethylcellulose (Sigma) was injected intraperitoneally into WT mice with the same time course as minocycline. For the inhibition of TLR9-dependent TNF-α production, mice were treated with thalidomide on day 1 after seizure and again the following day. To evaluate cell proliferation at each day, we injected BrdU into mice every 4 h (four times) at 1, 2, 3 and 4 days after KA administration and killed the mice 12 h after the last BrdU injection.

For the hippocampus-dependent recognition test, mice were transferred to the testing room and acclimated for at least 1 h before habituation and testing. Each mouse was habituated to the empty testing chamber (10 min) for 3 days after being handled for 3 days. The testing chamber was an opaque plastic chamber (50 × 50 × 30 cm). Two identical objects were placed in the testing chamber, and the mouse was allowed to explore the objects for 5 min as the training phase and then the mouse was taken out from the chamber. We then placed one of the two objects in a new position where is a diagonal corners with the object placed in familiar position (Fig. 5a). After a 5-min delay, the mouse was replaced in the testing chamber again. The mouse was given 5 min to explore the familiar and displaced objects during the testing phase. Behaviour was recorded with a video tracking system. Frequency of object interactions and time spent exploring each object were recorded for subsequent data analysis. The testing chamber and used objects were washed with 70% ethanol before the next mouse was tested. All mice were subjected to behavioural testing at 6 weeks after seizure.

All mice were treated according to Fundamental Guidelines for Proper Conduct of Animal Experiment and Related Activities in Academic Research Institutions under the jurisdiction of the Ministry of Education, Culture, Sports, Science and Technology of Japan.

Gene expression analysis. Total RNA was isolated from tissues and cells using Sepasol-RNA I Super G (Nacalai Tesque) following the manufacturer's instructions. RNA quality of all samples was checked by spectrophotometer. Reverse transcription reactions were carried out using the SuperScript *VILO* cDNA Synthesis Kit (Life Technologies) according to the kit protocol. Primer sequences used in this study can be found in Supplementary Table 1. qRT–PCR was performed with SYBR green fluorescent dye using Step One Plus (Applied Biosytems) and Mx3000 (Stratagene). GAPDH was used as an endogenous control to normalize samples.

Immunohistochemistry. We performed immunohistochemistry as described previously[41]. Briefly, male adult mouse brains were fixed in 4% paraformaldehyde and 40-μm sections were cut with a cryostat. For staining with anti-BrdU antibody,

brain sections were incubated for 15 min with 2 N HCl. The antibodies used were anti-BrdU (1:1,000, AbD Serotec), anti-DCX (1:500, Abcam), anti-CD68 (1:500, AbD Serotec), anti-Iba1 (1:500, Wako), anti-TLR9 (1:100, Imgenex), anti-GFAP (1:2,000, Millipore), anti-S100β (1:500, Sigma), anti-GFP (1:500, Aves Labs) and anti-NeuN (1:500, Millipore). Nuclei were stained using bisbenzimide H33258 fluorochrome trihydrochloride (Hoechst) (Nacalai Tesque).

Immunocytochemistry. Cells were fixed in 4% paraformaldehyde and processed for immunostaining as described[41]. Cells were stained with one of the following antibodies: anti-Iba1 (1:500, Abcam), anti-GFAP (1:500, Millipore), anti-active caspase3 (1:500, R&D Systems), anti-BrdU (1:500, AbD Serotec), anti-p65 (1:500, Abcam) and anti-CD11b (1:500, AbD Serotec). For anti-BrdU staining, fixed cells were incubated with 2 N HCl for 5 min. EdU staining was performed using the Click-iT EdU Alexa Fluor 555 Imaging Kit (Life Technologies) according to the supplier's protocol. Stained cells were visualized with a fluorescence microscope (Zeiss Axiovert 200M, Zeiss).

Confocal imaging. Fluorescence images were obtained on a confocal laser microscope (LSM710 and LSM780, Zeiss). For quantification of the percentage of NS/PCs contacted by microglia, Z-series stacks of confocal images of GFP-expressing Sox2-positive cells and Iba1-positive cells were taken. At least 50 randomly chosen GFP-positive cells in the DG per animal were analyzed. GFP-positive cells whose cell bodies contacted microglial processes or cell bodies were counted. For analysis of neuronal localization in the DG at 8 days after seizure, Z-series stacks of confocal images of DCX-positive cells with Hoechst staining were taken to determine the localization of DCX-positive cells. For analysis of dendritic complexity and measurement of dendrite length *in vivo*, three-dimensional reconstructions of the entire dendritic processes of individual DCX-positive neurons were made from Z-series stacks of confocal images as previously described[42]. Briefly, images were acquired at 0.5-μm intervals. The projection images were traced and analyzed with ImageJ. At least 10 randomly chosen DCX-positive cells in the DG per animal were analyzed. Sholl analysis for dendritic complexity was performed by counting the number of dendrites that crossed a series of concentric circles at 10-μm intervals from the cell soma.

Cell counts. BrdU-positive cells within the DG were counted using every 6th section (240 μm apart). The number of counted cells was then multiplied by six to provide an accurate estimation of the number of cells per DG. To calculate the total number of marker-double-positive cells, at least 200 randomly chosen BrdU-positive cells per animal were analyzed. Microscopic analysis yielded a ratio of BrdU-positive cells colabelled with DCX, NeuN, GFAP and S100β. These ratios were multiplied by the total number of BrdU-labelled cells to give estimates of the total number of BrdU-positive immature or mature neurons and BrdU-positive astrocytes. To estimate the ratio of surviving cells after seizure, the total number of BrdU-positive cells at 3 weeks post injection of BrdU was divided by the total number of BrdU-positive cells at day 1 post injection of BrdU.

Cell culture. We obtained primary microglia and astrocytes from mouse at postnatal day 1 (P1) using a previously described protocol[43], with some modifications. To obtain mixed glial cell cultures, cortexes of WT and TLR9-KO mice were carefully dissected after stripping of meninges. The tissue was digested with papain (Sigma) at 37 °C for 20 min. After centrifugation (200*g*, 5 min), the cell pellet was resuspended in alpha-Minimum Essential Medium (MEM) with 5% foetal bovine serum (FBS) and 0.6% glucose, and the suspension was passed through a 40-μm Cell Strainer (BD Falcon). After centrifugation (200*g*, 5 min), the cell pellet was resuspended in DMEM containing 10% FBS and a low concentration of GM-SCF (0.1 ng ml^{-1}; PeproTech) to enhance microglial proliferation. These mixed glial cells were plated in poly-L-lysine-coated T75 tissue culture flasks. The medium was renewed every 2–3 days. Ten days after plating, microglia and oligodendrocyte precursor cells (OPCs) were detached from astrocyte monolayer sheets by shaking, collected and plated onto uncoated 35-mm culture dishes to remove OPCs. After a 30-min incubation, the medium was removed by suction and DMEM containing 10% FBS without GM-SCF was added to the dish. Two days after plating, primary microglia from WT and TLR9-KO mice were used for assays.

After the shake-off procedure for the isolation of microglia, Trypsin EDTA solution (Nacalai Tesque) was added to the flask to obtain the remaining astrocytes, which were transferred to a 35-mm culture dish and maintained in DMEM containing 10% FBS. Two days after plating, the astrocytes were used for assays.

Neuronal cultures were prepared from P1 mouse hippocampus according to a previously described protocol[44], with some modification. In brief, the hippocampus was digested with papain at 37 °C for 20 min and triturated with a 1-ml pipette. MEM with 5% FBS and 0.6% glucose was added and the mixture was plated onto a poly-L-lysine-coated 35-mm culture dish. After 3 h, the medium was replaced with maintenance medium (Neurobasal Medium (Gibco) supplemented with B27 (Gibco)) containing cytosine β-D-arabinofuranoside (5 μM; Sigma) to eliminate proliferating cells. To avoid neuronal cell death by a complete medium change, half of the medium was replaced every 3 days with fresh maintenance medium. After 12 days, the neurons were used for assays.

To obtain NS/PCs, P1 mouse hippocampus was dissected and triturated in Hank's balanced salt solution. After centrifugation (200*g*, 5 min), the cell pellet was resuspended in N2-supplemented DMEM/F-12 medium containing 10 ng ml^{-1} bFGF (PeproTech), plated on a poly-L-ornithine/fibronectin-coated dish and incubated for 4 days. The cells were passaged by replating on an ornithine/fibronectin-coated dish in N2 medium with 10 ng ml^{-1} each of bFGF and EGF (PeproTech)[45]. NS/PCs that had been passaged 10 times were used for qRT–PCR analysis.

aNS/PC proliferation assay. For the *in vitro* aNS/PC proliferation assay, we used aNS/PCs derived from rat hippocampus as previously described[46]. To determine the effect of candidate cytokines, aNS/PCs were cultured in the presence of murine TNF-α, murine IL-12 and murine IFN-γ (all PeproTech) for 3 days. N2-supplemented DMEM/F-12 medium containing bFGF (5 ng ml^{-1}) was used as culture medium in this assay.

Cell supernatant collection. To analyze the role of microglia in aNS/PC proliferation, microglia obtained from WT mice were cultured in the presence or absence of ODN1585 (0.3 μM; InvivoGen), ODN1826 (1 μM; InvivoGen) and ODN2395 (1 μM; InvivoGen) for 3 h and washed with PBS. DMEM containing 10% FBS was added to microglial cultures and incubated for 21 h. CM was then collected. aNS/PCs were cultured with 30% microglial CM for 3 days. For the aNS/PC proliferation assay, either BrdU or EdU was added (to 10 μM) to the culture medium 30 min before fixation. For TNF-α neutralization experiments, microglial CM was supplemented with 10 μg ml^{-1} anti- mouse TNF-α (R&D Systems) or 10 μg ml^{-1} normal goat IgG as a control and incubated at 37 °C for 1 h before it was added to the aNS/PC culture.

To confirm microglial activation by endogenous ligand derived from neurons, neurons were cultured in the presence or absence of KA (100 μM) for 1 h and washed with Neurobasal Medium. To avoid neuronal cell death caused by a complete medium change, we then added a 1:1 mixture of fresh and used maintenance medium, which is CM from cultured neurons without any stimulation. After 24 h, we collected the CM. Primary microglia were treated with 30% neuronal CM. To determine whether endogenous ligand derived from degenerating neurons was DNA, CM from KA-treated neurons was pre-incubated with 50 μg ml^{-1} of DNase (Roche) at 37 °C for 1 h. For NF-κB activation analysis, primary microglia were treated with 30% CM from unstimulated or KA-stimulated neurons. Microglia cultured with the CM were stained with anti-p65 antibody. The TLR9 agonist ODN1826 was added to primary microglia as a positive control to induce the translocation of p65 protein into the nucleus. To determine whether NF-κB is activated by TLR9 signalling, microglia were pretreated with TLR9 antagonist (ODN2088) for 1 h before addition of CM and the translocation of p65 into the nucleus was examined.

Osmotic pump infusion. In murine TNF-α-infusion experiments, KA-treated TLR9-KO mice were infused with recombinant TNF-α (120 ng per day; PeproTech) into the right ventricle by osmotic minipumps (Alzet) for 5 days with the following coordinates: posterior = 0.34 mm from Bregma, lateral = 1 mm, ventral = 3 mm, as previously described[47].

Evans blue injection. A 2% solution of Evans blue dye (Sigma) in 0.9% NaCl was intravenously injected into WT and TLR9-KO mice in a dose of 2 ml kg^{-1} at 3 days after seizure. All mice were killed 3 h after the Evans blue injection.

Statistical analysis. Statistical comparisons were made by Student's *t*-test (for two-group comparisons) and analysis of variance (for multiple group comparisons) with Tukey *post-hoc* tests. Data represent mean + s.e.m.

References

1. Aimone, J. B., Deng, W. & Gage, F. H. Adult neurogenesis: integrating theories and separating functions. *Trends Cogn. Sci.* **14,** 325–337 (2010).
2. Ming, G. L. & Song, H. Adult neurogenesis in the mammalian brain: significant answers and significant questions. *Neuron* **70,** 687–702 (2011).
3. Parent, J. M. *et al.* Dentate granule cell neurogenesis is increased by seizures and contributes to aberrant network reorganization in the adult rat hippocampus. *J. Neurosci.* **17,** 3727–3738 (1997).
4. Lugert, S. *et al.* Quiescent and active hippocampal neural stem cells with distinct morphologies respond selectively to physiological and pathological stimuli and aging. *Cell Stem Cell* **6,** 445–456 (2010).
5. Okamoto, M. *et al.* Reduction in paracrine Wnt3 factors during aging causes impaired adult neurogenesis. *FASEB J.* **25,** 3570–3582 (2011).
6. Snyder, J. S., Soumier, A., Brewer, M., Pickel, J. & Cameron, H. A. Adult hippocampal neurogenesis buffers stress responses and depressive behaviour. *Nature* **476,** 458–461 (2011).
7. Song, J. *et al.* Neuronal circuitry mechanism regulating adult quiescent neural stem-cell fate decision. *Nature* **489,** 150–154 (2012).

8. Tremblay, M. E. *et al.* The role of microglia in the healthy brain. *J. Neurosci.* **31,** 16064–16069 (2011).
9. Nimmerjahn, A., Kirchhoff, F. & Helmchen, F. Resting microglial cells are highly dynamic surveillants of brain parenchyma *in vivo*. *Science* **308,** 1314–1318 (2005).
10. Saijo, K. & Glass, C. K. Microglial cell origin and phenotypes in health and disease. *Nat. Rev. Immunol.* **11,** 775–787 (2011).
11. Sierra, A. *et al.* Microglia shape adult hippocampal neurogenesis through apoptosis-coupled phagocytosis. *Cell Stem Cell* **7,** 483–495 (2010).
12. Gebara, E., Sultan, S., Kocher-Braissant, J. & Toni, N. Adult hippocampal neurogenesis inversely correlates with microglia in conditions of voluntary running and aging. *Front. Neurosci.* **7,** 145 (2013).
13. Sultan, S., Gebara, E. & Toni, N. Doxycycline increases neurogenesis and reduces microglia in the adult hippocampus. *Front. Neurosci.* **7,** 131 (2013).
14. Kawai, T. & Akira, S. The role of pattern-recognition receptors in innate immunity: update on Toll-like receptors. *Nat. Immunol.* **11,** 373–384 (2010).
15. Maroso, M. *et al.* Toll-like receptor 4 and high-mobility group box-1 are involved in ictogenesis and can be targeted to reduce seizures. *Nat. Med.* **16,** 413–419 (2010).
16. Laird, M. D. *et al.* High mobility group box protein-1 promotes cerebral edema after traumatic brain injury via activation of toll-like receptor 4. *Glia* **62,** 26–38 (2014).
17. Rolls, A. *et al.* Toll-like receptors modulate adult hippocampal neurogenesis. *Nat. Cell Biol.* **9,** 1081–1088 (2007).
18. Jessberger, S. *et al.* Epigenetic modulation of seizure-induced neurogenesis and cognitive decline. *J. Neurosci.* **27,** 5967–5975 (2007).
19. Kron, M. M., Zhang, H. & Parent, J. M. The developmental stage of dentate granule cells dictates their contribution to seizure-induced plasticity. *J. Neurosci.* **30,** 2051–2059 (2010).
20. Avignone, E., Ulmann, L., Levavasseur, F., Rassendren, F. & Audinat, E. Status epilepticus induces a particular microglial activation state characterized by enhanced purinergic signaling. *J. Neurosci.* **28,** 9133–9144 (2008).
21. Kobayashi, K. *et al.* Minocycline selectively inhibits M1 polarization of microglia. *Cell Death Dis.* **4,** e525 (2013).
22. Vallieres, L., Campbell, I. L., Gage, F. H. & Sawchenko, P. E. Reduced hippocampal neurogenesis in adult transgenic mice with chronic astrocytic production of interleukin-6. *J. Neurosci.* **22,** 486–492 (2002).
23. Iosif, R. E. *et al.* Tumor necrosis factor receptor 1 is a negative regulator of progenitor proliferation in adult hippocampal neurogenesis. *J. Neurosci.* **26,** 9703–9712 (2006).
24. Goshen, I. *et al.* Brain interleukin-1 mediates chronic stress-induced depression in mice via adrenocortical activation and hippocampal neurogenesis suppression. *Mol. Psychiatry* **13,** 717–728 (2008).
25. Han, X. *et al.* Forebrain engraftment by human glial progenitor cells enhances synaptic plasticity and learning in adult mice. *Cell Stem Cell* **12,** 342–353 (2013).
26. Koyama, R. *et al.* GABAergic excitation after febrile seizures induces ectopic granule cells and adult epilepsy. *Nat. Med.* **18,** 1271–1278 (2012).
27. Zhang, Q. *et al.* Circulating mitochondrial DAMPs cause inflammatory responses to injury. *Nature* **464,** 104–107 (2010).
28. Kawai, T. & Akira, S. Signaling to NF-κB by Toll-like receptors. *Trends Mol. Med.* **13,** 460–469 (2007).
29. Hemmi, H. *et al.* A Toll-like receptor recognizes bacterial DNA. *Nature* **408,** 740–745 (2000).
30. Oka, T. *et al.* Mitochondrial DNA that escapes from autophagy causes inflammation and heart failure. *Nature* **485,** 251–255 (2012).
31. Lehmann, S. M. *et al.* An unconventional role for miRNA: let-7 activates Toll-like receptor 7 and causes neurodegeneration. *Nat. Neurosci.* **15,** 827–835 (2012).
32. Liu, H. Y. *et al.* TLR7 negatively regulates dendrite outgrowth through the Myd88-c-Fos-IL-6 pathway. *J. Neurosci.* **33,** 11479–11493 (2013).
33. Trevejo, J. M. *et al.* TNF-α-dependent maturation of local dendritic cells is critical for activating the adaptive immune response to virus infection. *Proc. Natl Acad. Sci. USA* **98,** 12162–12167 (2001).
34. McCoy, M. K. & Tansey, M. G. TNF signaling inhibition in the CNS: implications for normal brain function and neurodegenerative disease. *J. Neuroinflammation* **5,** 45 (2008).
35. Nikolakopoulou, A. M., Dutta, R., Chen, Z., Miller, R. H. & Trapp, B. D. Activated microglia enhance neurogenesis via trypsinogen secretion. *Proc. Natl Acad. Sci. USA* **110,** 8714–8719 (2013).
36. Edwards, J. P., Zhang, X., Frauwirth, K. A. & Mosser, D. M. Biochemical and functional characterization of three activated macrophage populations. *J. Leukoc. Biol.* **80,** 1298–1307 (2006).
37. Miron, V. E. *et al.* M2 microglia and macrophages drive oligodendrocyte differentiation during CNS remyelination. *Nat. Neurosci.* **16,** 1211–1218 (2013).
38. D'Amour, K. A. & Gage, F. H. Genetic and functional differences between multipotent neural and pluripotent embryonic stem cells. *Proc. Natl Acad. Sci. USA* **100**(Suppl 1): 11866–11872 (2003).
39. Ziemann, A. E. *et al.* Seizure termination by acidosis depends on ASIC1a. *Nat. Neurosci.* **11,** 816–822 (2008).
40. Racine, R. J. Modification of seizure activity by electrical stimulation. II. Motor seizure. *Electroencephalogr. Clin. Neurophysiol.* **32,** 281–294 (1972).
41. Namihira, M. *et al.* Committed neuronal precursors confer astrocytic potential on residual neural precursor cells. *Dev. Cell* **16,** 245–255 (2009).
42. He, Y. *et al.* ALK5-dependent TGF-β signaling is a major determinant of late-stage adult neurogenesis. *Nat. Neurosci.* **17,** 943–952 (2014).
43. Giulian, D. & Baker, T. J. Characterization of ameboid microglia isolated from developing mammalian brain. *J. Neurosci.* **6,** 2163–2178 (1986).
44. Bekkers, J. M. & Stevens, C. F. Excitatory and inhibitory autaptic currents in isolated hippocampal neurons maintained in cell culture. *Proc. Natl Acad. Sci. USA* **88,** 7834–7838 (1991).
45. Abematsu, M. *et al.* Neurons derived from transplanted neural stem cells restore disrupted neuronal circuitry in a mouse model of spinal cord injury. *J. Clin. Invest.* **120,** 3255–3266 (2010).
46. Hsieh, J., Nakashima, K., Kuwabara, T., Mejia, E. & Gage, F. H. Histone deacetylase inhibition-mediated neuronal differentiation of multipotent adult neural progenitor cells. *Proc. Natl Acad. Sci. USA* **101,** 16659–16664 (2004).
47. Jang, M. H. *et al.* Secreted frizzled-related protein 3 regulates activity-dependent adult hippocampal neurogenesis. *Cell Stem Cell* **12,** 215–223 (2013).

Acknowledgements

We thank M. Yoshioka, I. Kirikae, J. Kohyama, N. Uezono, K. Ito, H. Tamura, S. Komai, S. Katada, T. Imamura and M. Namihira for experimental help and valuable comments. This work was funded by the Asahi Glass Foundation and a Grant-in-Aid for Exploratory Research from the Ministry of Education, Culture, Sports, Science and Technology of Japan (no. 24650198) and Core Research for Evolutional Science and Technology (CREST) from Japan Science and Technology Agency. T.M. received funding from a Sasakawa Scientific Research Grant and a Grant-in-Aid for JSPS Fellows (no. 13J09007).

Author contributions

T.M. contributed to the concept, design, execution and analysis of the experiments, provided funding and wrote the manuscript. N.M. contributed to the design and analysis of the experiments. Y.K. and B.J. contributed to analysis of the experiments. J.K., S.A. and T.K. provided advice and technical expertise. K.N. supervised the project and contributed to the concept and design of the experiments, provided funding and wrote the manuscript.

Additional information

Supplementary Information accompanies this paper at http://www.nature.com/naturecommunications

Competing financial interests: The authors declare no competing financial interest.

Reprints and permission information is available online at http://npg.nature.com/reprintsandpermissions/

How to cite this article: Matsuda, T. *et al.* TLR9 signalling in microglia attenuates seizure-induced aberrant neurogenesis in the adult hippocampus. *Nat. Commun.* 6:6514 doi: 10.1038/ncomms7514 (2015).

Molecular Brain

RESEARCH Open Access

Reprogramming non-human primate somatic cells into functional neuronal cells by defined factors

Zhi Zhou[1], Kazuhisa Kohda[1], Keiji Ibata[1], Jun Kohyama[1], Wado Akamatsu[1], Michisuke Yuzaki[1], Hirotaka James Okano[2], Erika Sasaki[1,3] and Hideyuki Okano[1*]

Abstract

Background: The common marmoset (*Callithrix jacchus*) is a New World primate sharing many similarities with humans. Recently developed technology for generating transgenic marmosets has opened new avenues for faithful recapitulation of human diseases, which could not be achieved in rodent models. However, the longer lifespan of common marmosets compared with rodents may result in an extended period for *in vivo* analysis of common marmoset disease models. Therefore, establishing rapid and efficient techniques for obtaining neuronal cells from transgenic individuals that enable *in vitro* analysis of molecular mechanisms underlying diseases are required. Recently, several groups have reported on methods, termed direct reprogramming, to generate neuronal cells by defined factors from somatic cells of various kinds of species, including mouse and human. The aim of the present study was to determine whether direct reprogramming technology was applicable to common marmosets.

Results: Common marmoset induced neuronal (cjiN) cells with neuronal morphology were generated from common marmoset embryonic skin fibroblasts (cjF) by overexpressing the neuronal transcription factors: *ASCL1*, *BRN2*, *MYT1L* and *NEUROD1*. Reverse transcription-polymerase chain reaction of cjiN cells showed upregulation of neuronal genes highly related to neuronal differentiation and function. The presence of neuronal marker proteins was also confirmed by immunocytochemistry. Electrical field stimulation to cjiN cells increased the intracellular calcium level, which was reversibly blocked by the voltage-gated sodium channel blocker, tetrodotoxin, indicating that these cells were functional. The neuronal function of these cells was further confirmed by electrophysiological analyses showing that action potentials could be elicited by membrane depolarization in current-clamp mode while both fast-activating and inactivating sodium currents and outward currents were observed in voltage-clamp mode. The 5-bromodeoxyuridine (BrdU) incorporation assay showed that cjiN cells were directly converted from cjFs without passing a proliferative state.

Conclusions: Functional common marmoset neuronal cells can be obtained directly from embryonic fibroblasts by overexpressing four neuronal transcription factors under *in vitro* conditions. Overall, direct conversion technology on marmoset somatic cells provides the opportunity to analyze and screen phenotypes of genetically-modified common marmosets.

Keywords: Common marmoset, Direct reprogramming, Induced neuronal cells, Transcription factor, Regenerative medicine, Disease modeling, Cell-fate plasticity, Transdifferentiation

* Correspondence: hidokano@a2.keio.jp
[1]Department of Physiology, Keio University School of Medicine, 35 Shinanomachi, Shinjuku-ku, Tokyo 160-8582, Japan
Full list of author information is available at the end of the article

Background

The common marmoset (*Callithrix jacchus*) is a New World primate that has recently attracted considerable attention as a non-human primate model for biomedical research [1]. Specific features of the common marmoset are its small size, ease of handling, high fertility, early sexual maturity, its similarity of physiological properties with humans, drug metabolism, and neurophysiological functions [1]. Thus far, transgenic mice modeling human neurodegenerative diseases have contributed to disease research and drug development. However, none of them have succeeded in faithfully recapitulating the full spectrum of disease pathologies observed in humans [2,3]. In a recent report by our group, transgenic marmosets with germline transmission were successfully generated for the first time by lentiviral vector-mediated gene transfer [4]. For these reasons, our novel transgenic non-human primate models may be suitable for studying human diseases, particularly those that are neurodegenerative, such as Alzheimer's and Parkinson's disease. These *in vivo* models are expected to faithfully recapitulate pathophysiology of human diseases, and thus provide for the missing link between mouse and human disease research with subsequent drug development. However, results of studies from these models may require an extended period because of the longer lifespan of common marmosets compared with mice [5]. Moreover, detailed *in vitro* analyses using primary neuronal cultures of the affected area of the common marmoset transgenic models are not realistic.

Recent studies using human neuronal cells derived from either pluripotent stem cells or somatic cells have succeeded in modeling human neurological disorders *in vitro* [6,7]. These results prompted us to develop a convenient and rapid method for obtaining common marmoset neuronal cells from accessible somatic cells. Therefore, we focused on somatic cell reprogramming technology, including induced pluripotent stem (iPS) cell and direct conversion technology [8,9]. However, few studies have succeeded in generating common marmoset iPS cells from neonatal skin fibroblasts, fetal liver cells, and adult bone marrow-derived cells [10-12]. Moreover, only a few protocols exist for obtaining functional common marmoset neuronal cells from pluripotent stem cells [13]. Furthermore, little attention has been given to the direct conversion technology of common marmoset dermal fibroblasts into neuronal cells thus far. Therefore, in the present study, we aimed to generate common marmoset neuronal cells directly from dermal fibroblasts. Our results provide the first line of evidence for the generation of electrophysiologically functional neuronal cells from common marmoset somatic cells by defined neuronal transcription factors.

Results and discussion

Validation of the lentivirus-mediated overexpression of neuronal transcription factors

Recently, generation of induced neuronal (iN) cells was reported using mouse and human dermal cells [9,14]. In the present study, we used a set of neuronal transcription factors for human iN cells on common marmoset embryonic skin fibroblasts (cjF) isolated from embryonic day 91 (E91) embryos to determine whether common marmoset somatic cells could be converted into neuronal cells. We first confirmed transgene expression in the mouse fibroblast cell line, NIH3T3, by infecting these cells with lentiviral vectors coding the neuronal transcription factors: *ASCL1*, *BRN2*, *MYT1L*, and *NEUROD1* [14], under the control of tetracycline response element (TRE) together with reverse tetracycline transactivator (rtTA)-expressing vector. Upregulation of transgenes in NIH3T3 cells after doxycycline (dox) treatment was confirmed by immunocytochemistry (Additional file 1).

Generation of neuron-like cells from common marmoset somatic cells

To address whether cjFs, which were immunonegative for the neural progenitor marker, SRY (sex determining region Y)-box 2 (Sox2) (data not shown), can be converted into cjiN cells, cjFs were infected with these lentiviral vectors at 0 day *in vitro* (div) (Figure 1A). Synapsin reporter-positive mouse iN cells have been shown to be more functionally mature than negative cells [15]. Therefore, the reporter lentivirus, which expresses fluorescent protein (enhanced green fluorescent protein or DsRed) under the control of the human synapsin I promoter, was used in the present study to monitor neuronal conversion of cjFs [16-18] (Figure 1A). When cjFs were treated with dox at 1 div to induce neuronal conversion (Figure 1B), synapsin reporter-positive cells with typical neuronal morphologies were observed (Figure 2A, B). However, cjFs without dox treatment did not generate synapsin reporter-positive cells (Figure 2A). Notably, the morphology of synapsin reporter-positive cells resembled fibroblasts at 9 div and then changed into neuronal ones during reprogramming (Figure 2A, B). The reprogramming efficiency was monitored by the number of synapsin reporter-positive cells with neuronal morphology, and depended on the concentration of dox yielding 0.3 ± 0.1, 21.8 ± 0.8, or 32.6 ± 2.6 cjiN cells/cm^2 at 16 div when treated with 0, 1, or 2 μg/mL dox, respectively (Figure 2C) ($P^{***} < 0.001$, $P^{\#\#} < 0.01$, n = 4). However, the overall induction efficiency was much lower (<1%) than those in previous studies using mouse and human fibroblasts [9,14]. This discrepancy was probably due to the low infection efficiency of lentivirus in cjFs compared with those in mouse and human fibroblasts. Previous studies have also shown that polycistronic vector, micro RNAs and small molecules can facilitate iN cell induction

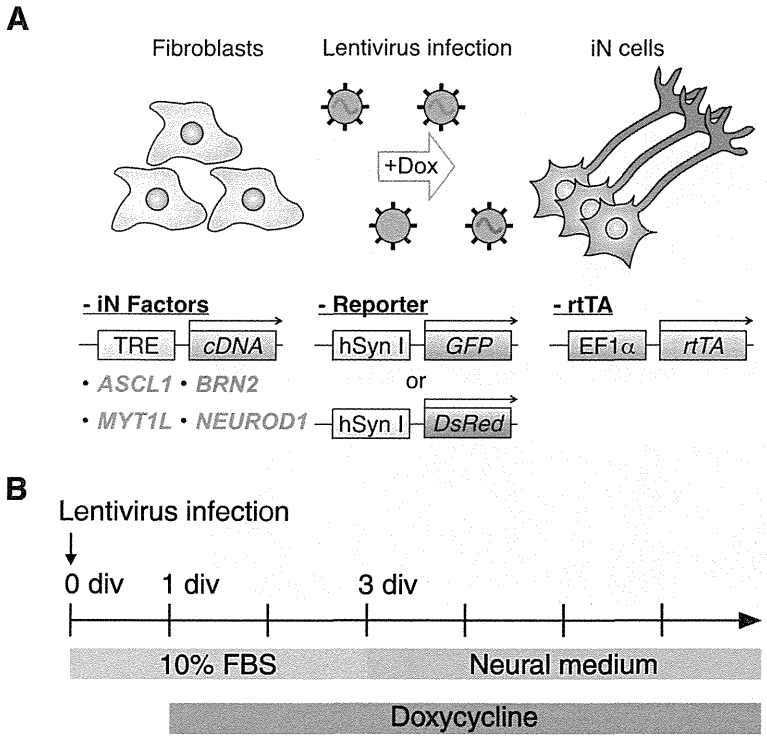

Figure 1 Schematic overview of the experimental procedure for generation of common marmoset induced neuronal cells from common marmoset embryonic skin fibroblasts. (A) Common marmoset embryonic skin fibroblasts (cjFs) were infected with drug-inducible lentiviral vectors coding a set of induced neuronal (iN) cell factors: *ASCL1*, *BRN2*, *MYT1L*, and *NEUROD1*. Synapsin reporter lentivirus expressing green fluorescent protein (GFP) or DsRed under the human synapsin I promoter was used to monitor neuronal induction. The lentiviral vector that stably drives *rtTA* expression under the EF1α promoter was transduced to induce the expression of iN-factors. **(B)** Time course for common marmoset induced neuronal (cjiN) cell induction. Lentivirus infection was conducted at 0 day *in vitro* (div) in fibroblast medium containing 10% fetal bovine serum, and cells were exposed to doxycycline (dox) at 1 div for cjiN induction. The culture medium was then replaced at 3 div with dox-containing neural meium composed of N2B27 medium, neurotrophin-3 (NT-3) and brain-derived neurotrophic factor (BDNF). For calcium imaging, the cAMP analog, 8-(4-Chlorophenylthio) adenosine 3′, 5′-cyclic monophosphate (8-CPT; 100 μM) [29], was added to promote neuronal maturation and survival.

[7,19,20]. Therefore, the induction conditions of cjiN cells may be optimized in the future study to enhance the conversion efficiency. Nevertheless, our results show that the four-factor set of neuronal transcription factors is sufficient to convert cjFs to cjiN cells.

The duration of dox treatment was critical for neuronal conversion

Next, we investigated the required duration of exogenous neuronal transcription factor expression to drive neuronal transdifferentiation. Therefore, we examined the exposure time of dox and the cjiN induction efficiency (Figure 2D). Treatment with dox from 1–3 div promoted the conversion of cjFs into synapsin reporter-positive cells with neuronal morphology (Figure 2E). Similarly, a previous study has shown that the endogenous neuronal transcriptional factor network is activated 48 h after dox treatment [14]. Our findings also revealed that the induction efficiency at 23 div depended on the exposure time of dox (Figure 2F). The treatment of cjFs with dox from 1–11 div followed by a culture without dox treatment from 11–23 div generated 112.1 ± 28.1 cjiN cells/cm^2 (Figure 2F). However, cells cultured with dox from 1–3 div followed by a culture without dox treatment from 3–23 div generated only 10.6 ± 5.4 cjiN cells/cm^2 (Figure 2F). The efficiency of the former group was significantly ($P^{***} < 0.001$, n = 4) higher (more than 10-fold) compared with the latter group (Figure 2F). These results indicate that a longer expression of exogenous neuronal transcriptional factors is required for efficient lineage conversion of somatic cells.

cjiN cells expressed a subset of neuronal genes and proteins

To characterize cjiN cells as neuronal cells, we performed reverse transcription-polymerase chain reaction (RT-PCR) analysis using bulk RNA samples, including the remaining synapsin reporter-negative cells to explore the expression of neuronal genes (see Table 1 for the primer sets used). We detected an upregulation of neuronal genes (Figure 3), which included cytoskeletal markers

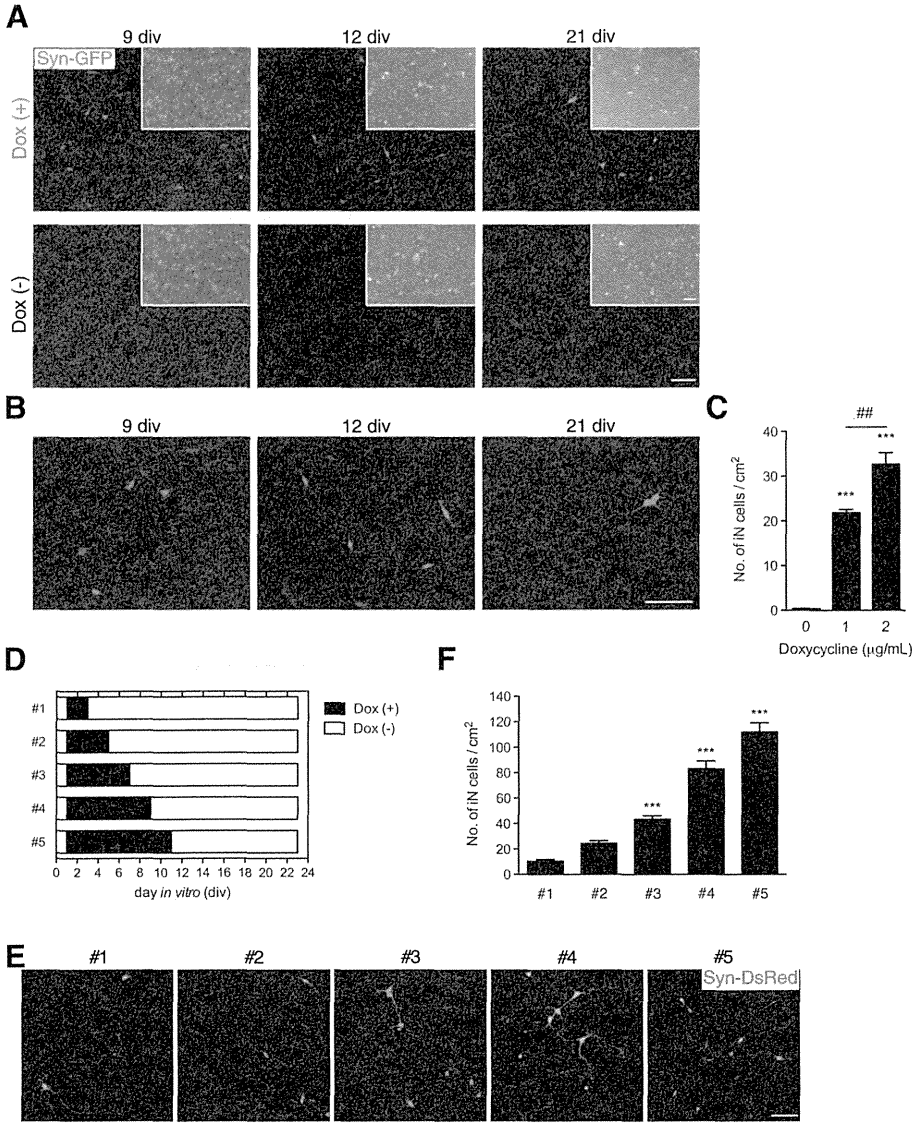

Figure 2 Generation of iN cells. (A, B) Transgene-dependent conversion of common marmoset fibroblasts into neuronal cells, in which synapsin reporter activation and morphological changes were dependent on the exogenous transcription factor and time. Cells became synapsin reporter-positive accompanied by a gradual morphological changes into neuronal cells, both effects of which were not found in cells cultured in neural medium without dox at 21 div. **(B)** Magnified images of Figure 1A showing synapsin reporter-positive cells with morphological changes from fibroblasts to neuronal cells. **(C)** Counts of synapsin reporter-positive cells with neuronal morphology showed a dox-dependent increase in their number (positive cells with fibroblast morphology were excluded from the counts). $P^{***} < 0.001$, $P^{\#\#} < 0.01$ (one-way ANOVA followed by Tukey's test). **(D-F)** The effect of sustained dox treatment on the production of cjiN cells. **(D)** Cells were treated with dox at 1 div until 3, 5, 7, 9 or 11 div and then maintained without dox until 23 div. **(E)** Synapsin reporter-positive cells with neuronal morphology were observed in all treatment group. **(F)** Cell counts revealed that a longer treatment time of dox increased the number of cjiN cells. Although dox treatment from 1–3 div sufficiently promoted cjiNs, a longer treatment time increased their number. $P^{***} < 0.001$ (one-way ANOVA followed by Tukey's test). Scale bar; 200 μm.

(*MAP2*, *DCX* and *TUBB3*), synaptic vesicle markers (*SYN1* and *VGLUT1*), and cation channel-related genes (*SCN1A*, *GRIN1* and *GRIA1*) in cjiN cells at 21 div (Figure 3). However, expression of these neuronal genes was not detected in cjFs at 0 div (Figure 3). These results were in line with the concentration-dependent induction efficiency of dox in Figure 2C. We also detected endogenous expression of *BRN2* and *NEUROD1* in cjiN cells at 21 div (Figure 3), indicating that ectopic expression of neuronal transcription factors activated the endogenous neuronal program. This effect may have caused neuronal transdifferentiation from somatic cells [9,14,21]. Thus, ectopic neuronal differentiation

Table 1 Primer sets used in RT-PCR analysis

Gene name	Forward primer	Reverse primer	Product size (bp)
SYN1	acggagactaccgcagtttg	cgatctgctccagcattgca	459
DCX	ctgtgcgtgtgcttctgaac	tcagctggagacttgcttcg	346
TUBB3	catagaccccagtggcaactacg	caccctccgtgtagtggcccttgg	241
MAP2	cctgtgttaagcggaaaacc	agagactttgtcctttgcctgt	86
VGLUT1	tcaataacagcacgacccac	tcccggaatttgagtgacaatg	131
SCN1A	attggcaattccgtgggagc	cccacacagcacgcggaaca	204
GRIN1	accccaagatcgtcaacatcg	ggctaaccagaatggcgtaga	213
GRIA1	cgagctttcctgttgatacat	tctgccacttgtaatggtcgatg	99
endo BRN2	aattaaggaaaaaggaaagcaact	caaaacatcattacacctgct	71
endo NEUROD1	gttattgtgttgccttagcacttc	agtgaaatgaattgctcaaattgt	77
ACTB	ggcatccacgaaactacctttt	acactgagtacttgcgctcg	202

signals are likely to work together with the endogenous neuronal program to efficiently convert non-neuronal cells into neuronal cells [21].

To further characterize the property of cjiN cells, we performed immunocytochemistry for the neuronal markers. The results showed that most synapsin reporter-positive cells also expressed (>88%) the pan-neuronal marker, microtubule-associated protein 2 (MAP2) (data not shown). This result indicated that the synapsin reporter using the sequence of human synapsin I promoter was also functional in common marmoset cells, and was thus a reliable reporter for neuronal conversion, as previously reported [15,16]. In cjiN cells at 43 div, MAP2-negative cells were found to be negative for glial fibrillary acidic protein and only weakly positive for α-smooth muscle actin (data not shown), raising the possibility that they were partially reprogrammed cells. The MAP2- and synapsin reporter-positive cells also showed immunoreactivity for the synaptic vesicle marker, synaptophysin, at 38 div (Figure 4A). However, immunostaining for synaptophysin and PSD95 revealed that these cells were unlikely to make synapse structures at 38 div (data not shown). Although the cjiN cells expressed neuronal marker genes and proteins, they did not appear to be mature enough to make synaptic contacts themselves. However, a future study may facilitate synaptic formation by improving induction efficiency and by co-culturing with astrocytes [9,14].

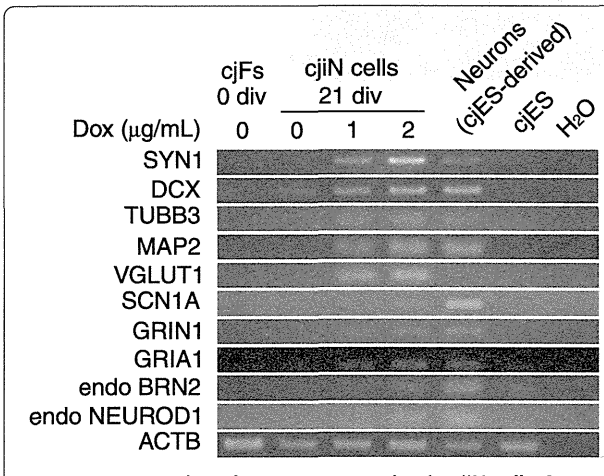

Figure 3 Neuronal marker gene expression in cjiN cells. Dox treatment upregulated cytoskeletal (*MAP2*, *DCX*, and *TUBB3*) and synaptic vesicular (*SYN1* and *VGLUT1*) marker genes, and cation channel-related genes (*SCN1A*, *GRIN1* and *GRIA1*). The results also showed the activation of endogenous *BRN2* and *NEUROD1* genes.

The majority of cjiN cells were glutamatergic

To characterize the neurotransmitter phenotype of iN cells, we examined the expression of neurotransmitters in MAP2-positive cjiN cells. Immunostaining at 38 div for vesicular glutamate transporter 1 (vGlut1) and gamma aminobutyric acid (GABA) revealed the presence of both excitatory glutamatergic and inhibitory GABAergic neuronal cells, respectively (Figure 4B). Counts of vGlut1 and GABA-positive cjiN cells showed a significantly ($P^{***} < 0.001$, n = 4) greater number of vGlut1-positive cells (39.2 ± 1.9/cm^2) than GABA-positive cells (16.4 ± 2.8 cells/cm^2) (Figure 4C). These results are in accordance with previous studies showing that the majority of iN cells are excitatory cells [7,14,22]. Our findings thus indicate that iN induction may be feasible in the future for the *in vitro* analysis of the transgenic common marmoset model of Alzheimer's disease, in which forebrain excitatory neurons are expected to be affected. Moreover, our cjiN cell induction protocol is likely advantageous over the previously reported neuronal differentiation protocol which used common marmoset embryonic stem (ES) cells and iPS cells, because the ES/iPS cell-derived neural precursor cells showed caudal identity [13]. Thus far, several groups have succeeded in generating reprogrammed neuronal cells with specific neuronal subtypes, such as dopaminergic neurons and motor neurons [23-26], which implicate the cell fate plasticity of terminally differentiated somatic cells.

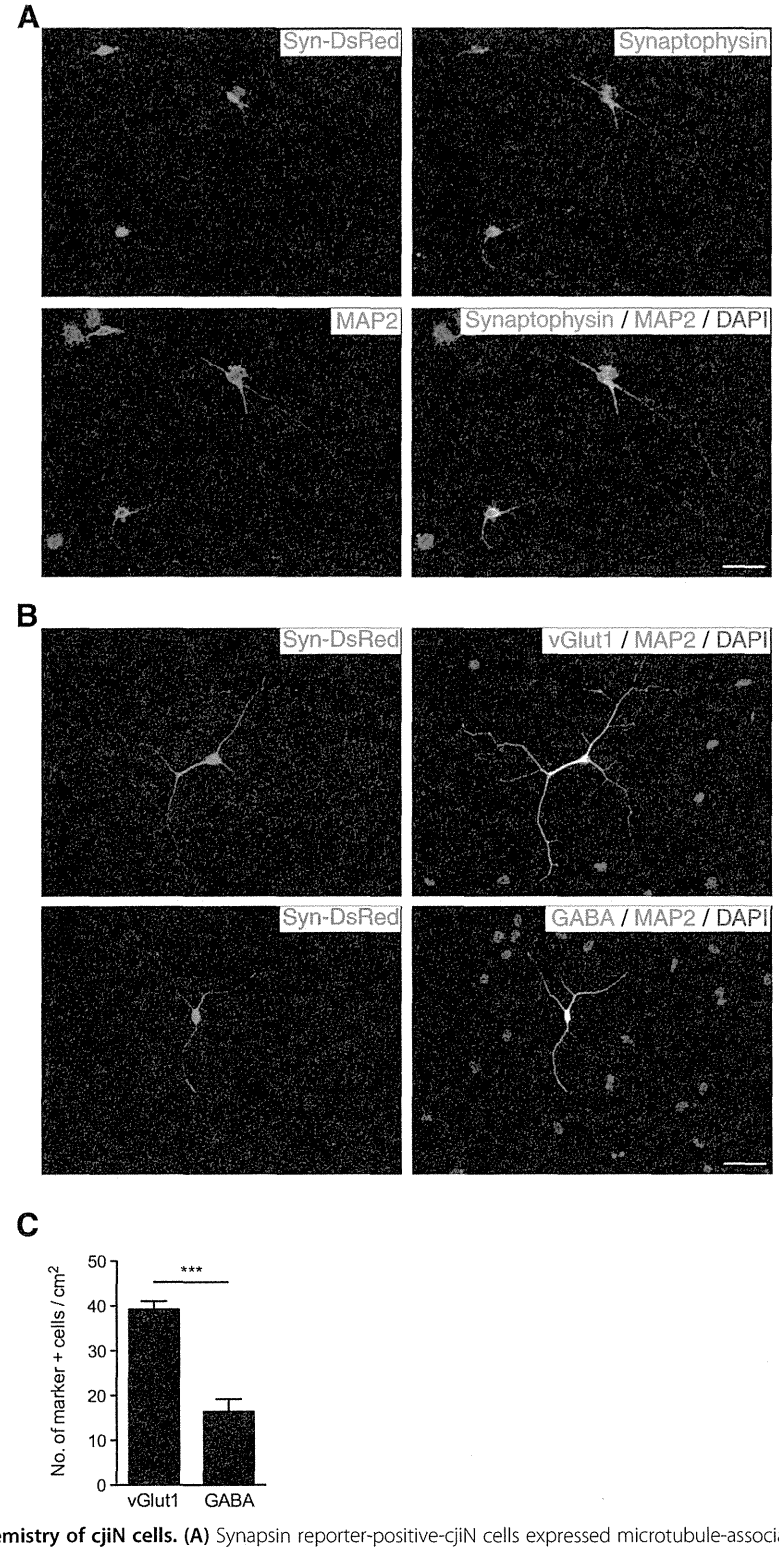

Figure 4 Immunocytochemistry of cjiN cells. (A) Synapsin reporter-positive-cjiN cells expressed microtubule-associated protein 2 (MAP2) and synaptophysin. **(B)** cjiN cells were vesicular glutamate transporter 1 (vGlut1)- and gamma-aminobutyric acid (GABA)-positive, thereby displaying a heterogeneous pool of excitatory and inhibitory neurons, respectively. **(C)** A significantly greater number of vGlut1-positive cells was generated compared with GABA-positive cells. $P^{***} < 0.001$ (Student's *t*-test). Scale bar; 50 μm.

Our success in reprogramming common marmoset somatic cells into excitatory and inhibitory neuronal cells using defined iN factors may therefore provide great promise in the future for generating specific subtypes of neuronal cells with specific sets of neuronal transcription factors.

cjiN cells were functional as matured neurons

To further confirm the successful conversion of cjFs into functional neuronal cells, we performed calcium imaging analysis. cjiN cells cultured with dox were incubated with the calcium indicator, Fluo-4 AM [13], followed by response recordings. The intracellular calcium level ($[Ca^{2+}]_i$) in cjiN cells at 15 div was increased in cjiN cells perfused with 80 mM of KCl, which was then decreased by washout (Additional file 2). Furthermore, electrical field stimulation on cjiN cells at 28 div increased $[Ca^{2+}]_i$, which was reversibly blocked by the voltage-gated sodium channel blocker, tetrodotoxin (0.2 μM) (Figure 5), suggesting that the increase in $[Ca^{2+}]_i$ was likely evoked by action potentials through voltage-gated sodium channels. These results showed that cjiN cells derived from cjFs were functionally comparable to common marmoset ES cell-derived neuronal cells [13], and thus strongly suggest that reprogramming of common marmoset somatic cells generates functional neuronal cells. Moreover, electrophysiological analyses of cjiN cells at 29–42 div revealed that action potentials were elicited by membrane depolarization in current-clamp mode in 17 out of 21 cjiN cells (81.0%) (Figure 6A and Additional file 3). Among these 17 cjiN cells, 7 cjiN cells (41.2%) generated a single action potential and the remaining 10 cjiN cells (58.8%) generated repetitive action potentials (Figure 6A and Additional file 3). In the voltage-clamp mode, both fast-activating and inactivating sodium currents and outward currents were observed (Figure 6B). The resting membrane potentials of cjiN cells ranged between -26 and -55 mV, with a mean ± SEM of -38.1 ± 2.0 mV (Figure 6C and Additional file 3). This mean value was significantly ($P^{***} < 0.001$) lower than that of cjFs (-16.4 ± 0.6 mV) with a range between -13.1 and -19.0 mV (Figure 6C and Additional file 3). Overall, our patch clamp recordings showed that cjiN cells are functional neuronal cells.

cjiN cells were directly converted from cjFs without passing through a proliferative state

To determine whether cjiN cells were directly converted from cjFs without passing through a proliferative neural

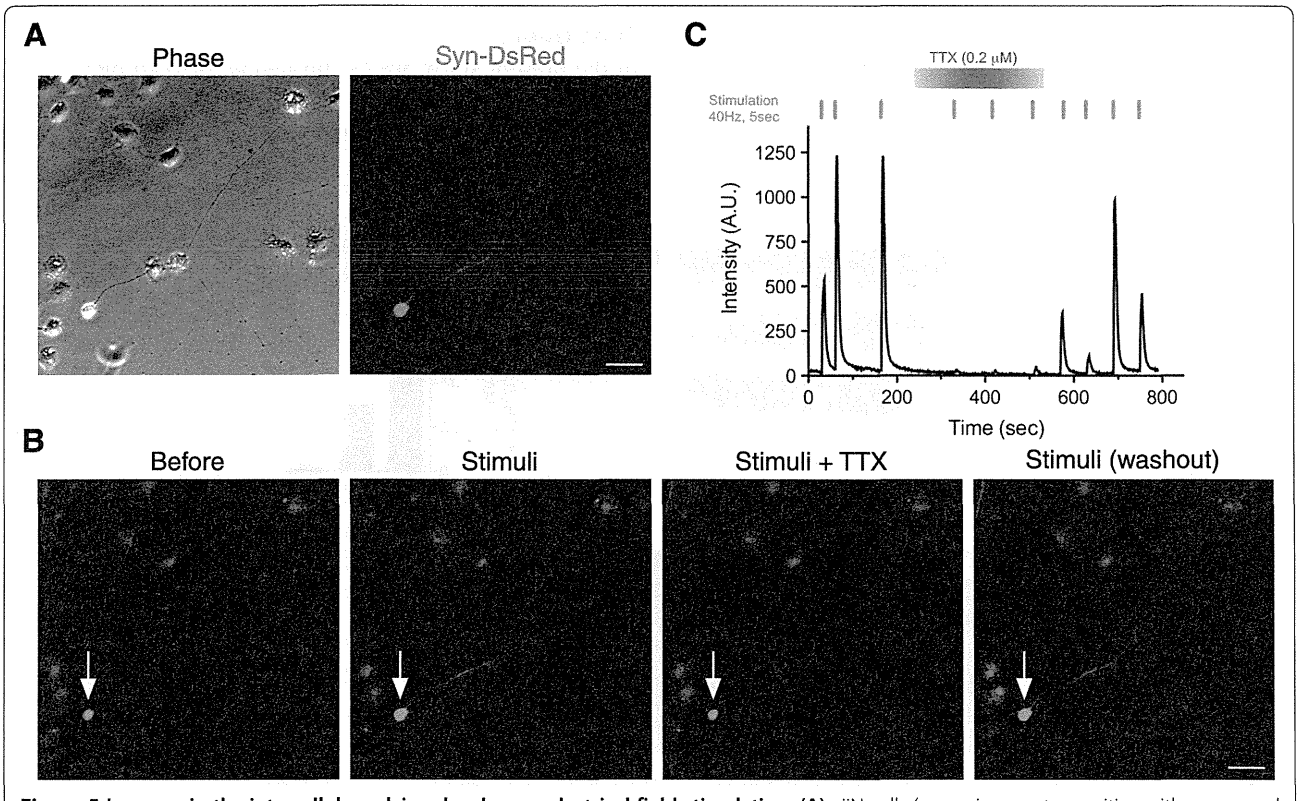

Figure 5 Increase in the intracellular calcium level upon electrical field stimulation. (A) cjiN cells (synapsin reporter-positive with a neuronal morphology). **(B, C)** Intracellular calcium level ($[Ca^{2+}]_i$) in cjiN cells was measured by the intensity of Fluo-4 fluorescence. Electrical field stimulation (40 Hz for 5 seconds) induces a robust elevation of $[Ca^{2+}]_i$ in some synapsin reporter-positive cells. The increase in $[Ca^{2+}]_i$ was reversibly suppressed by the specific voltage-gated sodium channel blocker, tetrodotoxin. Scale bar; 50 μm.

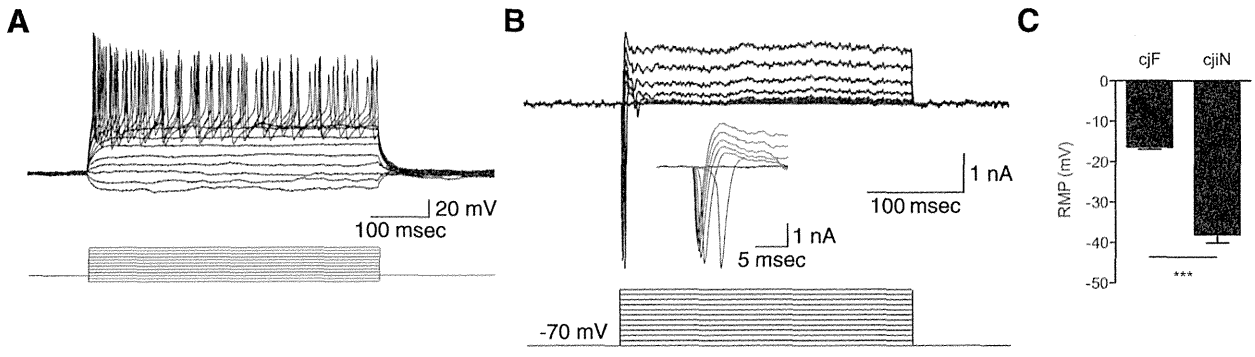

Figure 6 Neuronal electrophysiological property of cjiN cells. (A) cjiN cells elicited repetitive action potential by membrane depolarization in current-clamp mode. **(B)** cjiN cells showed both fast-activating and inactivating sodium currents and outward currents in voltage-clamp mode. **(C)** cjiN cells exhibited significantly lower resting membrane potentials than cjFs. $P^{***} < 0.001$ (Mann-Whitney *U*-test).

progenitor-like cell state, 5-bromodeoxyuridine (BrdU; 10 μM) was added to the media at 1, 3 or 5 div until 24 div (Figure 7A), and the percentage of double-positive cells for BrdU and MAP2 among the MAP2 single-positive cells was determined (Figure 7B, C). The result showed that while 85.3 ± 5.4% of MAP2-positive cells incorporated BrdU when treated from 1–24 div, only 30.1 ± 9.0% ($P^{**} < 0.01$) and 1.5 ± 1.5% ($P^{***} < 0.001$) of MAP2-positive cells incorporated BrdU when treated from 3–24 and 5–24 div, respectively (Figure 7C). This result indicates that most of the cells that were destined to be cjiN cells became postmitotic at the early phase of the reprogramming process, suggesting that cjiN induction is a direct process unless cells pass through a proliferative neural progenitor-like cell state, from which neuronal cells can be differentiated. In the present study, however, no Sox2-positive cells were found during 2–5 div, while MAP2-positive cells were present at 21 div (data not shown), indicating that the induction of neural progenitor-like cells is unlikely during 1-5 div. Therefore, these results show that cjiN cells are directly converted from cjFs without passing through proliferative neural progenitor cells.

Conclusions

In the present study, we established an *in vitro* method to convert common marmoset somatic cells into functional neuronal (i.e. cjiN) cells. The majority of the cjiN cells were

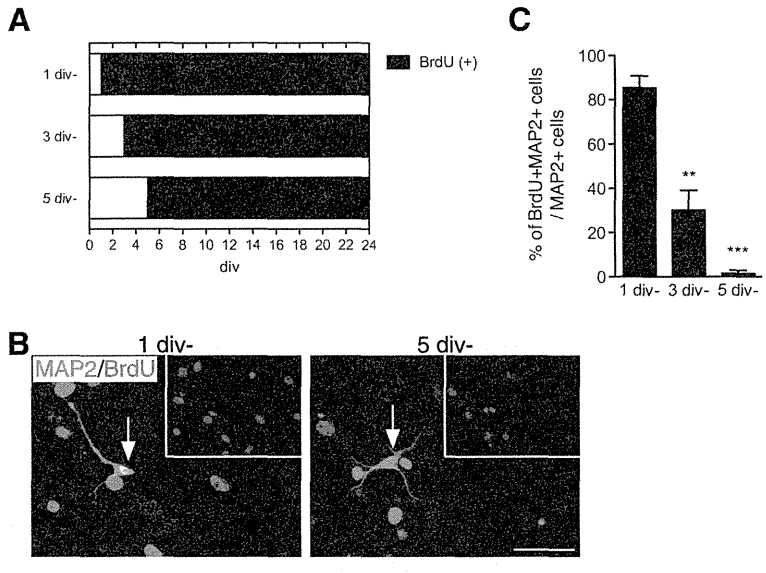

Figure 7 Cells destined to be cjiN cells became postmitotic at the early phase of the reprogramming process. (A) Time course for the BrdU incorporation experiment. BrdU (10 μM) was added into the culture medium at 1, 3 or 5 div until cells were fixed at 24 div. **(B, C)** Immunocytochemistry against MAP2 and BrdU revealed that when cells were treated with BrdU at 1 div until 24 div, 85.2 ± 5.4% of cjiN cells were BrdU + MAP2+, while when treated at 3 or 5 div until 24 div, only 30.1 ± 9.0% or 1.5 ± 1.5% of cjiN cells were BrdU + MAP2+, respectively, showing that the cjFs became postmitotic soon after transgene expression. $P^{***} < 0.001$ $P^{**} < 0.01$. Scale bar; 50 μm.

vGlut1-positive excitatory neuronal cells and expressed the neuronal marker genes: *TUBB3*, *DCX*, *MAP2*, *SYN1*, *VGLUT1*, *SCN1A*, *GRIN1* and *GRIA1*. Importantly, cjF-derived cjiN cells exhibited functional neuronal properties and responded to exogenous stimulation. Overall, these findings suggest that direct conversion technology may be beneficial in rapid and robust screening of neuronal phenotypes of transgenic common marmoset models of human diseases and analyzing underlying molecular mechanisms of diseases.

Methods

Animals

All animal experiments were approved by the Institutional Animal Care and Use Committee of the Central Institute for Experimental Animals (CIEA), and was performed in accordance with CIEA and Keio University guidelines.

Cell culture

Common marmoset embryonic fibroblasts, NIH3T3 cells and 293T cells were cultured in Dulbecco's modified Eagle's medium supplemented with 10% fetal bovine serum, 100 U/mL of penicillin and 100 μg/mL of streptomycin (10% FP medium) at 37°C with 5% CO_2 incubation.

Molecular cloning and lentivirus production

cDNA entry clone of human *ASCL1* [GenBank: NM_004316] was purchased from DNAFORM (clone ID: 100006383, Japan). cDNAs of human *BRN2* [GenBank: NM_005604.3], *MYT1L* [GenBank: NM_015025.2] and *NEUROD1* [GenBank: NM_002500.4] were cloned into pENTR-D-TOPO vector (Invitrogen, USA). Then cDNAs were inserted into a self-inactivation human immunodeficiency virus-1-based lentivirus construct, CSIV-TRE-RfA (CSIV-TRE-RfA-CMV-KT was kindly provided by Dr. Hiroyuki Miyoshi (RIKEN BRC, Japan), and then modified by Dr. Takuji Maeda (Nagoya University, Japan)), by LR reaction (Invitrogen, USA). Similarly, reverse tetracycline transactivator (rtTA) gene was inserted into CSII-EF1α-RfA-TK-HygR construct [27]. The human synapsin I reporter constructs, pCSC-hSynI-GFP [16] and pHIV7-hSynI-DsRed [18], were kindly provided by Dr. Fred H. Gage, Salk Institute, USA, and Dr. Alysson R. Muotri, University of California, USA, respectively. Besides, CSIV-hSynI-GFP-IRES2-NeoR and CSIV-hSynI-DsRed-IRES2-NeoR were constructed in-house. These reporters were constructed using CSIV-TRE-RfA-CMV-KT, pCSC-hSynI-GFP, pHIV7-hSynI-DsRed and pIRESneo3 (Clontech, USA) with PCR- and restriction enzyme-based method. For lentivirus production, 293T cells were transfected with lentivirus plasmid, pCAG-HIVgp and pCMV-VSV-G-RSV-Rev [28] (kindly provided by Dr. Hiroyuki Miyoshi, RIKEN BRC, Japan). After 16-20 h, supernatant was replaced by fresh media followed by 48-72 h incubation. The virus containing media were then collected and 0.45 μm-filterated followed by ultracentrifugation. The concentrated virus was suspended in PBS and used in subsequent experiments.

Induction of common marmoset iN cells

Common marmoset embryonic fibroblasts were seeded directly on culture ware at 1×10^4 cells/cm^2. Twenty-four hours later, the cells were infected with lentivirus in 10% FP media containing polybrene (8 μg/mL) (Sigma-Aldrich, USA). After 16–20 h in media containing lentivirus, the cells were switched into fresh 10% FP medium containing doxycycline (dox) (2 μg/mL) to drive transgene expression. Procedures for experiments determining the sufficient concentration and duration of dox are shown in the main text. After 48 h in 10% FP media with dox, the media was replaced with dox-containing neural media composed of N2B27 media [20], brain-derived neurotrophic factor (BDNF) (10 ng/mL, R&D systems, USA) and neurotrophin-3 (NT-3) (10 ng/mL, R&D systems, USA). For calcium imaging, 8-(4-Chlorophenylthio) adenosine 3′, 5′-cyclic monophosphate (8-CPT, 100 μM, Sigma-Aldrich, USA), one of the cAMP analogs [29], was also supplemented to promote neuronal maturation. The media was changed every 2–3 days during culture period. BrdU incorporation assay was performed as previously described [9] incubating cells with BrdU (10 μM, BD, USA) until cells were fixed.

Immunocytochemistry

Cells were fixed with 4% paraformaldehyde for 15 minutes at room temperature and then processed for immunocytochemistry [13]. Samples were rinsed with PBS three times. Then, samples were incubated at 4°C overnight with the primary antibodies diluted in PBS containing 5% of fetal bovine serum and 0.3% Triton X-100. The primary antibodies used were as follows; Synaptophysin (1:50000, Millipore, USA), MAP2 (1:1000, Sigma-Aldrich, USA), MAP2 (1:500, Millipore, USA), vGlut1 (1:2000, Synaptic systems, Germany), GABA (1:1000, Sigma-Aldrich, USA), PSD95 (1:500, Millipore, USA), α-SMA (1:500, Sigma-Aldrich, USA), Sox2 (1:500, R&D, USA), Ascl1 (1:200, BD, USA), Brn2 (1:200, Santa Cruz, USA), Myt1L (1:500, Abcam, England) and NeuroD1 (1:500, Santa Cruz, USA). After three washes with PBS, samples were incubated with secondary antibodies conjugated with Alexa-488, Alexa-555 and Alexa-647 (Invitrogen, USA). Nuclei were counterstained with 4′, 6-diamidino-2-phenylindole (DAPI; 1:1000, Dojindo, Japan). After washing with PBS, samples were mounted on slides with FluorSave reagent (Calbiochem, Germany) and examined under a universal fluorescence microscope (Axioplan 2; Carl Zeiss, Germany). For anti-BrdU staining (1:500, Abcam, England), cells were treated with 1 N HCl in PBS for 30 minutes at

37°C and then rinsed with PBS three times before primary antibody incubation.

RNA isolation and reverse transcription-polymerase chain reaction (RT-PCR)

Total RNA was isolated with RNeasy Micro Kit with DNase I treatment (QIAGEN, Germany) and was used to synthesize cDNA with ReverTraAce qPCR RT Kit (TOYOBO, Japan) according to the manufacturer's instruction. RT-PCR was conducted using Ex Taq HS (TAKARA, Japan) according to the manufacturer's instruction. Common marmoset ES (cjES) cells and cjES-derived neurons were used as control [13]. The primer sets used are listed in Table 1.

Calcium imaging and electrical stimulation

Calcium imaging analyses were performed as described previously [13]. To load the calcium imaging dye, cells were incubated with 1 μM Fluo-4 AM (Invitrogen, USA) in imaging solution consisting of 117 mM NaCl, 2.5 mM KCl, 2 mM $CaCl_2$, 2 mM $MgSO_4$, 25 mM HEPES and 30 mM D-(+)-glucose, (pH 7.4), at 37°C for 20 minutes, followed by washing for 30 minutes in imaging solution. Coverslips were placed on a custom-made field stimulation chamber and mounted on the stage of a Nikon Eclipse microscope with a 20× (NA 0.45) objective. Cells were perfused at 2 ml/minute with the imaging solution at room temperature with or without 0.2 μM tetrodotoxin (TTX; Alomone Labs Ltd., Israel). Images were acquired at 2 Hz (500 millisecond exposure time) with a cooled CCD camera (Andor iXon, DU897). Extracellular field stimulation was performed with two parallel platinum wires at 25 V/cm. Each stimulation was a train of 500 microsecond pulses at 40 Hz for 5 seconds. Images were analyzed with ImageJ software (NIH, Bethesda, MD).

Electrophysiology

Electrophysiological recordings were performed as described previously [30]. Synapsin reporter-positive cjiN cells were identified under an inverted microscope (Diaphot-TMD 200; Nikon, Japan) and whole cell patch clamp recordings were done using Axopatch 200B (Axon Instruments, USA) at room temperature. The extracellular solution composed of 117 mM NaCl, 2.5 mM KCl, 2 mM $CaCl_2$, 2 mM $MgCl_2$, 15 mM D-Glucose and 20 mM HEPES (pH 7.4 adjusted with NaOH, 304 mOsm) was continuously perfused during recordings. Patch pipettes had a resistance of 5-6 MΩ filled with the intracellular solution containing 130 mM K-gluconate, 1 mM $CaCl_2$, 1 mM $MgCl_2$, 10 mM EGTA, 10 mM Sucrose and 20 mM HEPES (pH adjusted with KOH, 305 mOsm). In voltage-clamp recordings, iN cells were held at -70 mV and voltage steps (10 mV, 300 msec) were applied to elicit voltage-activated currents. Action potentials were evoked by injecting step currents (20-40 pA, 500 msec) in the current-clamp mode. Data were digitized at 10 kHz with a 2 kHz low-pass filter. Liquid junction potential was corrected.

Statistical analysis

All data were expressed as means ± SEM. The statistical significance of differences was analyzed by Student's *t*-test, Mann-Whitney *U*-test or one-way ANOVA followed by Tukey's test using Graph Pad Prism5 software. Differences of $P < 0.05$ were considered statistically significant.

Additional files

Additional file 1: Doxycycline-dependent transgene induction in NIH3T3 cells. Immunocytochemistry against Ascl1, Brn2, Myt1L and NeuroD1 in a mouse fibroblast cell line, NIH3T3 cells, that were lentivirally transduced with iN factors and treated with doxycycline from 1–4 div revealed doxycycline-dependent transgene expressions. Scale bar; 100 μm.

Additional file 2: KCl perfusion increased the intracellular calcium level. (A) cjiN cells (synapsin reporter-positive with a neuronal morphology). **(B, C)** Intracellular calcium level ($[Ca^{2+}]_i$) in cjiN cells was measured by the intensity of Fluo-4 fluorescence. KCl (80 mM) perfusion caused a robust elevation of $[Ca^{2+}]_i$ in some synapsin reporter-positive cells. This increase was reversibly suppressed by washout. Scale bar; 50 μm.

Additional file 3: Electrophysiological parameters in cjiN cells at 29–42 div.

Abbreviations

cjiN cells: Common marmoset induced neuronal cells; cjF: Common marmoset embryonic fibroblast; RT-PCR: Reverse transcription-polymerase chain reaction; dox: Doxycycline; rtTA: Reverse tetracycline transactivator.

Competing interests

H.O. is a paid scientific consultant to San Bio, Inc., Eisai Co., Ltd., and Daiichi Sankyo Co., Ltd.

Authors' contributions

ZZ conceived the concept of this study, designed the experiments, performed experiments and analyzed data. KI, KK and MY performed calcium imaging assays and electrophysiology, and ZZ, KI, KK and MY analyzed data. JK, WA, HJO and HO coordinated the study. ES prepared and provided common marmoset embryonic fibroblasts. HO provided financial support for the experiments. ZZ, JK and HO wrote the paper. All authors read and approved the final manuscript.

Acknowledgements

We are grateful to memebers of Okano laboratory, Keio Unversity school of medicine for helpful advice and discussions. Dr. Hiroyuki Miyoshi, RIKEN BRC, Japan, kindly provided us with lentiviral vectors. Dr. Takuji Maeda, Nagoya University, Japan, kindly provided us with modified lentiviral vector. Dr. Fred H. Gage, Salk Institute, USA, and Dr. Alysson R. Muotri, University of California, USA, kindly provided us with synapsin reporter lentiviral vectors. This work is supported in part by a Grants-in Aid to Keio University from the Global COE Program of the Ministry of education, Culture, Sports, Science and Technology, Japan, Keio University Grant-in-Aid for Encouragement of Young Medical Scientists, and Funding Program for World-leading Innovative R&D on Science and Technology (FIRST) program of the Cabinet Office, Government of Japan and the Japan Society for the Promotion of Science (JSPS).